2002-03/06

Manaaki Whenua
Landcare Research

Recharge of Moutere aquifers: a report into investigations on recharge mechanisms

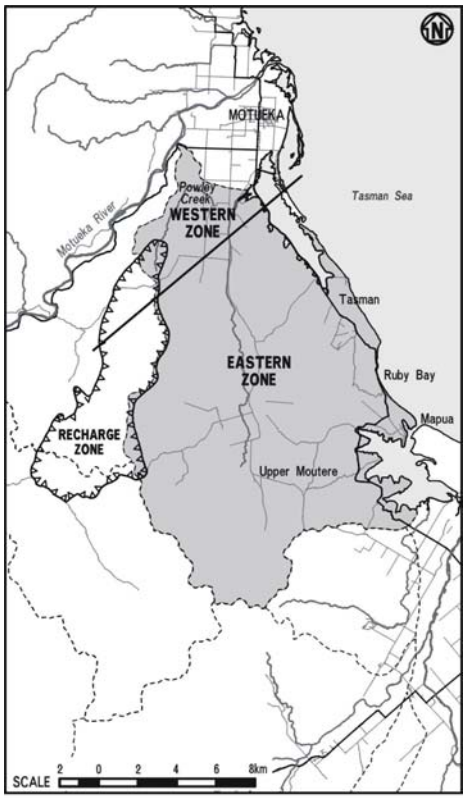

Prepared for

Stakeholders of the
Motueka Integrated Catchment Management Programme

Manaaki Whenua
Landcare Research

Tasman District Council

CAWTHRON

Institute of GEOLOGICAL & NUCLEAR SCIENCES Limited

June 2003

Recharge of Moutere aquifers: draft report into investigations on recharge mechanisms

Motueka Integrated Catchment Management
(Motueka ICM) Programme Report Series

by

T. Davie, R. Jackson, L. Basher, Landcare Research
M. Stewart, T. Hong, Institute of Geological & Nuclear Sciences
J. Thomas, Tasman District Council

NEW ZEALAND
Phone: 03 325 6700
Fax: 03 325 2418
Email: DavieT@LandcareResearch.co.nz

Cover Photo: Moutere groundwater zones.

PREFACE

An ongoing report series, covering components of the Motueka Integrated Catchment Management (ICM) Programme, has been initiated in order to present preliminary research findings directly to key stakeholders. The intention is that the data, with brief interpretation, can be used by managers, environmental groups and users of resources to address specific questions that may require urgent attentin or may fall outside the scope of ICM research objectives.

We anticipate that providing access to environmental data will foster a collaborative problem-solving approach through the sharing of both ICM and privately collected information. Where appropriate, the information will also be presented to stakeholders through follow-up meetings designed to encourage feedback, discussion and coordination of research objectives.

CHAPTER 1: INTRODUCTION

Groundwater in the Moutere Valley is an important resource for horticulture. Its use has increased from the middle 1980s, after deep wells revealed the hitherto unknown water resource. The hydrogeology of the groundwater system was investigated by Thomas (1989, 1991, 1992, 2001). The present work investigates the age of the groundwater and how recharge to the aquifers may be occurring in order to improve understanding of the nature of the system. This will lead to better understanding of the patterns and rates of recharge to the deep Moutere Aquifers, including its location and recent history. Better understanding of the groundwater system and recharge will contribute to policy on future permitted land uses in the recharge areas.

The groundwater system is largely unexplored, especially in the south of the area. The area has been divided into three zones for purposes of discussion: west, east and south (Fig.1). (The western and eastern zones are already used for management of the resource, Thomas 2001).

1.1 Hydrogeology

The Moutere Depression is a 30 km-wide system of valleys between the Tasman Mountains and the ranges of east Nelson. Voluminous Plio-Pleistocene gravels (including Moutere Gravel) are preserved in the depression and have been incised by the Motueka, Moutere and Waimea rivers (Rattenbury *et al*. 1998). Geophysical interpretation of seismic data and petroleum wells indicate the depression reaches depths of 2500 m on the eastern side (Lihou 1992). The depression formed in the Pliocene-Pleistocene during uplift of the Tasman Mountains and the east Nelson Ranges.

Moutere Gravel is a uniform yellow-brown, clay-bound gravel, with deeply weathered clasts almost entirely of Torlesse-derived sandstone and semi-schist. Well rounded, quartzofeldspathic sandstone clasts in a brown weathered muddy sand matrix comprise the bulk of the gravel.

Geological and geophysical investigations show the Moutere Valley as a NNE trending basinal basement structure. Integration of bore logs, down-hole geophysical logging and seismic profile data has enabled the recognition of three gravel units within the Moutere Gravel, i.e. basal, middle and upper. The Moutere Gravel units recognised are separated by generally clayey and sometimes carbonaceous zones. Geological and geophysical logging indicates cleaner and more compact gravels with depth. Surface geological mapping has enabled the recognition of two units of Moutere Gravel, the lower unit Moutere Gravel (tm1), and the upper unit Moutere Gravel (tm2). The above has been reinforced by microfloral age datings carried out by the DSIR which shows age differences for the basal and upper parts of the Moutere Gravel. The lower unit Moutere Gravel (tm1) outcrops only in the southeast of the area and dips gently into the Moutere Valley. The lower unit Moutere Gravel is correlated with the basal Moutere Gravel unit and the middle Moutere Gravel unit identified in the seismic reflection survey. The upper Moutere Gravel unit (tm2) mapped has been correlated with the upper Moutere Gravel unit identified in the seismic reflection survey.

Based on hydrogeological investigations, three aquifers have been delineated in the Moutere Valley, i.e. Deep Moutere Aquifer (DMA), Middle Moutere Aquifer (MMA) and shallow Moutere Aquifer (SMA). Hydrogeological data shows that the aquifer system is a leaky one, with there being a low permeability zone between the DMA and MMA and another between the MMA and SMA. The SMA is confined at the surface by reworked valley infilling. Groundwater yields improve significantly with depth with these parameters also strongly influenced by basement topography. Yields improve northwards and north-westwards from Ruby Bay. The deeper aquifers have better yields than the shallow one. A major fault identified from seismic analysis compartmentalizes the groundwater system in the area (Figure 1.1), into the Western Groundwater Zone and Eastern Groundwater Zone.

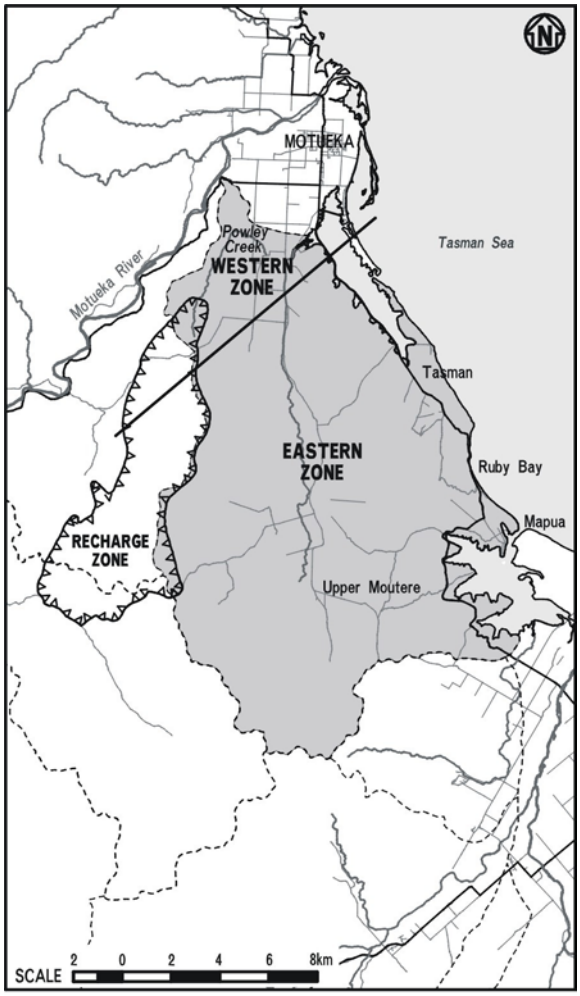

Figure 1.1: Moutere groundwater zones

1.2 Groundwater Recharge

Geological, geophysical and hydraulic data show that the southwest sector (Figure 1.2) of the Moutere Valley, where the lower unit Moutere Gravel (tm1) outcrops, is the principal recharge area for the deep aquifers (DMA, MMA) of the Moutere Valley. Groundwater recharge occurs by direct rainfall infiltration through unconfined sections of the aquifers (Figure 1.2).

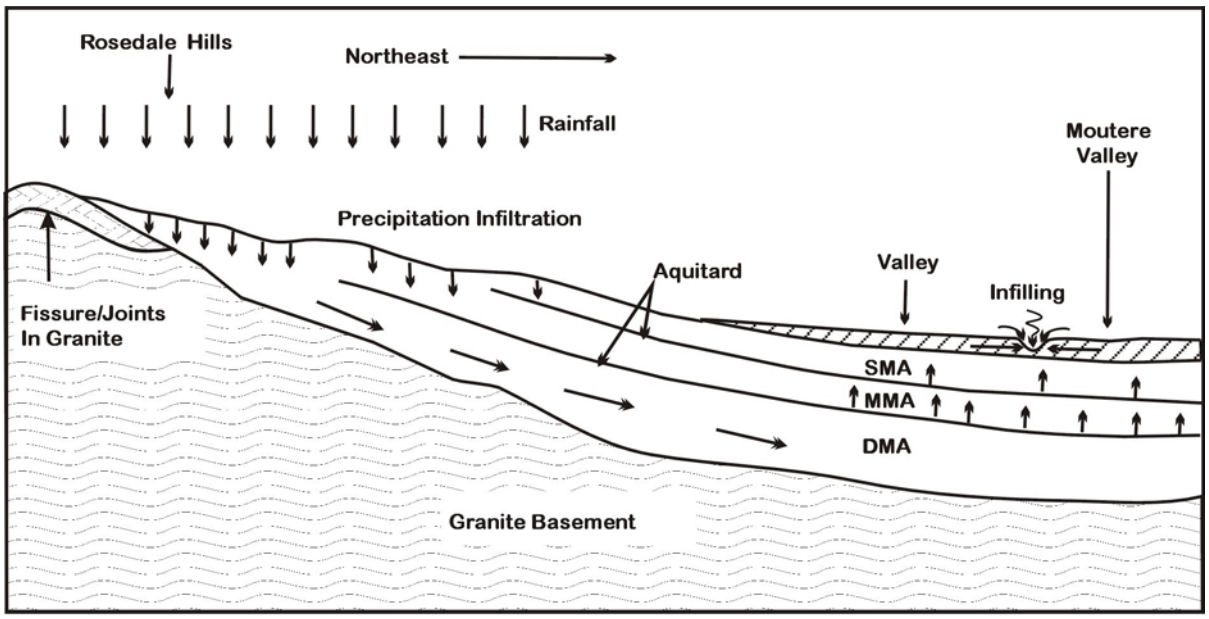

Figure 1.2: Schematic recharge model for the Moutere aquifers

1.3 Summary of Current Knowledge

All investigations carried out to date show a precipitation infiltration recharge to the deep Moutere Aquifers with the principal recharge coming from the southwestern sector of the area where the lower unit (tm1) Moutere Gravel outcrops. The surface boundary of the lower unit (tm1) Moutere Gravel was defined based on hydrogeological data (i.e. mapping and age datings).

1.4 Scope of Report

This report presents the results from three separate studies investigating groundwater recharge issues in the Moutere aquifer region.

Chapter 2 is a study that uses water chemistry and isotopes of carbon and oxygen to investigate the age of water derived from the Moutere aquifers and possible recharge mechanisms. The work was carried out by Dr Mike Stewart at the Institute of Geological and Nuclear Sciences, Lower Hutt , funded by FRST programme *Understanding Groundwater Sustainability* to GNS, and as part of the FRST funded *Integrated Catchment Management* programme of research.

Chapter 3 uses an empirical model of the Moutere aquifer system to investigate the response of the aquifers to abstraction. The work was carried out by Dr Timothy Hong at the Institute of Geological and Nuclear Sciences, Wairakei, as part of the FRST funded *Integrated Catchment Management* programme of research.

Chapter 4 presents the results from work investigating surface water balance processes in the groundwater recharge zone, within the Waiwhero catchment. This is a combination of field and modelling investigation. The work was carried out by staff at Landcare Research, Lincoln, led by Dr Rick Jackson and Dr Tim Davie, funded through contracts to Tasman District Council and as part of the FRST funded *Integrated Catchment Management* programme of research.

CHAPTER 2: ISOTOPES AND CHEMISTRY

The chapter presents work using isotopes and chemistry in conjunction with other data to investigate the nature and recharge of Moutere Valley groundwater.

2.1 Sampling and Methods

Sampling and bore details are given in Stewart (2002; table 1). The bore locations are shown in figure 2.1a.

Isotopic data

Groundwater wells were purged of at least three casing volumes before samples were taken. Bottles were flushed with the water to be sampled, emptied, and filled with water and allowed to overflow. Care was taken to seal the bottles tightly to prevent evaporation. Samples of water were collected in 28 mL glass bottles for ^{18}O, 500 mL bottles for carbon isotopes, and 1.1 L bottles for tritium.

For ^{18}O measurement, 2 mL of the water is isotopically equilibrated with CO_2 gas at 29^{o}C for two hours, and then the CO_2 is analysed in a stable isotope mass spectrometer (Hulston et al., 1981). For tritium, samples are distilled, enriched in tritium by electrolysis and then counted in a Quantalus low background liquid scintillation counter for several weeks (Hulston et al., 1981). Carbon isotope measurements are made by quantitatively extracting carbon from an aliquot of the water as CO_2 by adding acid. The total yield of CO_2 is measured. Part of the CO_2 is analysed for ^{13}C, the remainder is turned into a graphite target for accelerator mass spectrometric analysis of ^{14}C.

Chlorofluorocarbons

Water samples for CFC concentration measurements were collected in such a way as to prevent contact of the sample with the atmosphere or with plastic materials, either of which could contaminate the water with excess CFCs. The samples are preserved in the field by sealing them into 62 mL borosilicate glass ampoules at the well site. The sampling apparatus is connected to the well outlet by copper tubing. All other tubing in contact with the water during sampling is stainless steel. The ampoule is attached to the sampling apparatus and flushed with ultra-high-purity nitrogen gas. The well water is then allowed to flow through the tubing and valves and into the bottom of the ampoule, displacing the nitrogen. The ampoule is rinsed with several hundred millilitres of water, then nitrogen is forced into the neck to displace some of the water. The ampoule is then fused shut about 1-2 cm above the water level with an oxy/acetylene gas torch. Nitrogen flows continually across the union to prevent any air contamination. Four ampoules are normally collected at each sampling site. The CFC samples were analysed by gas chromatography.

Chemical data

Water samples have been collected from groundwater wells in the Moutere Valley by Tasman District Council hydrologists for a number of years. Samples for cations were field filtered and acidified with high-purity nitric acid. Samples for anions were field filtered and kept below 4°C until analysed, and bicarbonate samples were collected unfiltered, kept below 4°C, and analysed within 48 hrs of collection. Samples were analysed by the Cawthron Institute in Nelson. Analytical methods have changed for some parameters, but in general the same methods have been used for each collection period. Methods for cation analyses include Atomic Adsorption, ICP-OES, and for anion analyses include auto titrator, auto analyser, and ion chromatography.

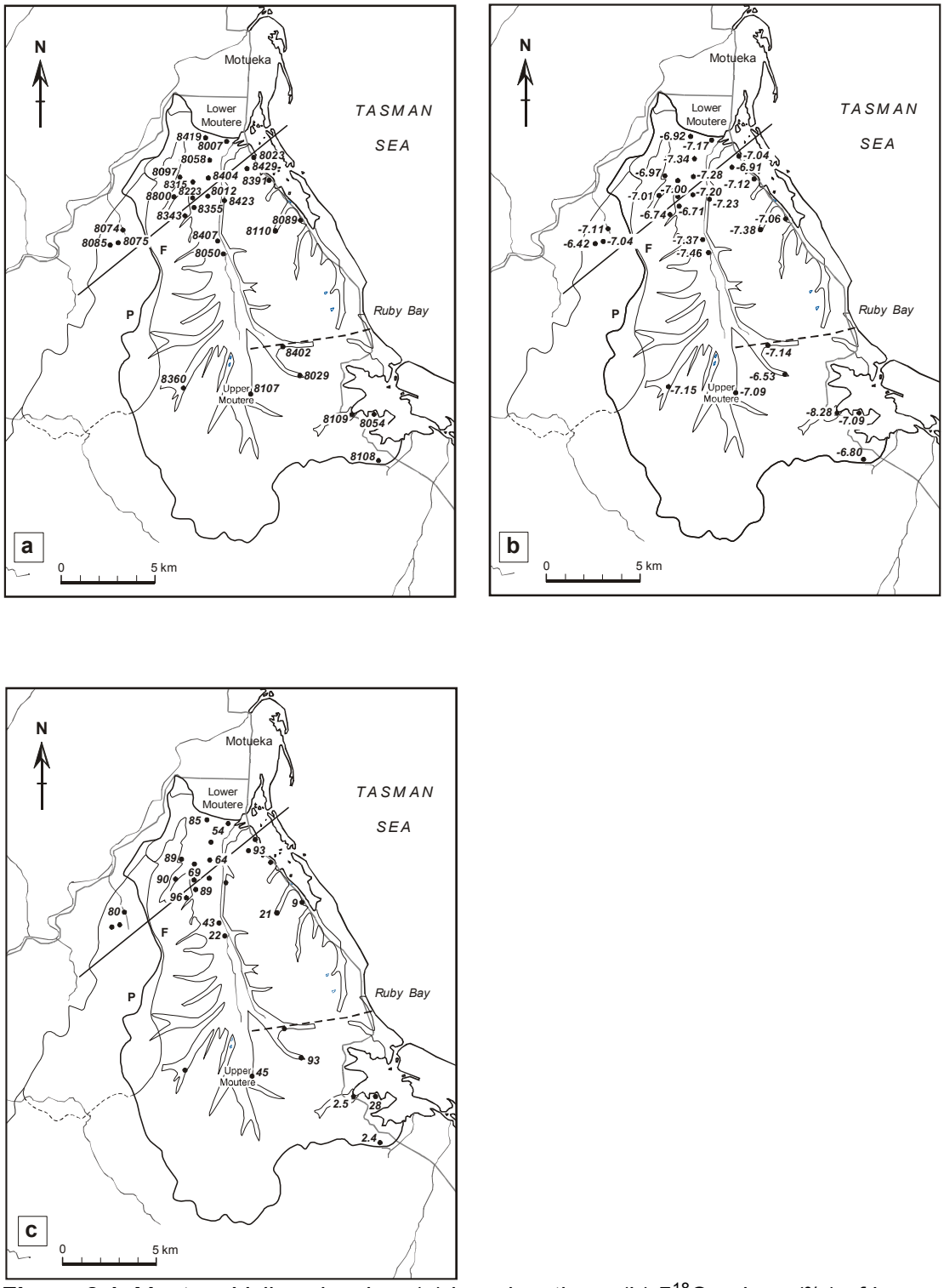

Figure 2.1: Moutere Valley showing: (a) bore locations, (b) $\delta^{18}O$ values (‰) of bore waters, and (c) ^{14}C concentrations (pmC) of bore waters.

2.2 Results

Oxygen-18 concentrations

$\delta^{18}O$ values give information on the source of the groundwater because there is generally a relationship between the location of recharge and its $\delta^{18}O$ value (Stewart and Morgenstern, 2001).

^{18}O concentrations in water are expressed as δ values with respect to a water standard in units of per mil (‰), where

$$\delta^{18}O\ (‰) = [(^{18}O/^{16}O)_{sample} / (^{18}O/^{16}O)_{VSMOW} - 1] \times 1000 \quad (1)$$

The standard (VSMOW or Vienna Standard Mean Ocean Water) is held at the International Atomic Energy Agency in Vienna. Measurement errors are ±0.1‰ (one standard deviation).

$\delta^{18}O$ in precipitation depends on altitude, latitude, and distance from the sea along prevailing storm tracks. The average relationships between $\delta^{18}O$ and altitude and latitude for New Zealand precipitation are expressed by the equations

$$\delta^{18}O = -0.0021h - 5.51 \quad (2)$$

$$\delta^{18}O = -0.22L + 3.58 \quad (3)$$

where h is the altitude in metres, and L the latitude South in degrees. This gives $\delta^{18}O$ of about –5.5‰ for precipitation at sea level and –6.2‰ for precipitation at 300-m altitude for Moutere. However, Moutere is situated east of the Tasman Mountains, which lie at right angles to the prevailing storm tracks from the west, and therefore precipitation at Moutere would be expected to be more negative than the above estimate. The mean $\delta^{18}O$ value of precipitation on the Waimea Plains at Richmond (near sea level) was measured at –6.2‰ (Stewart et al. 1981) and gives a guide to the values to be expected at Moutere. This would indicate values of –6.2‰ at sea level and –6.9‰ at 300-m altitude for the Moutere Valley.

Recent measurements of the mean $\delta^{18}O$ values of groundwater recharge from rainfall in comparison with the rainfall itself suggest that there can be differences between them (work in progress on Canterbury Plains; Stewart et al., 2002). If winter rainfall provides more of the recharge, because more water is lost by evapotranspiration in summer, then the $\delta^{18}O$ of the recharge will be more negative than the $\delta^{18}O$ of the rainfall. Monthly rainfall measurements at Waiwhero and Rosedale had annual mean values of –6.3‰, and winter mean values of –7.1‰. Nearby pasture and forest springs had mean values of –6.4‰ and –6.6‰ respectively. These indicate a probable range for rainfall-recharged groundwater in the region of –6.4 to –7.1‰.

In fact, the $\delta^{18}O$ values of the Moutere Gravel groundwaters are in the range –6.4 to –7.5‰, except for one bore with $\delta^{18}O$ of -8.3‰. (The latter is discussed below).

The $\delta^{18}O$ values show interesting areal patterns (Figure 2.1b). In the western zone, the shallow bores on the west side of the valley (i.e. the Waiwhero area, bores WWD8074, 8075, 8085) have $\delta^{18}O$ values of –7.0 to –7.1‰. (8085 is an open well, so its value of –6.4‰ is likely to have been affected by evaporation.) On the west side of the valley floor, bores WWD 8419, 8364, 8097, 8800 and 8223 have values of about –6.9 to –7.0‰. These waters are likely to have been recharged in the Waiwhero area. The remaining bores in the valley floor WWD8007, 8058 and 8404 tap deeper waters and have more negative $\delta^{18}O$ values (–7.2 to –7.3‰). (Well 8404 has been sampled since 1988 and has shown no change in $\delta^{18}O$ in that time).

In the eastern zone, shallow bores on the west side of the Moutere Valley (WWD8343 and 8355) have $\delta^{18}O$ values of –6.7 to –6.8‰. The deeper bores within the valley floor (WWD8012, 8423, 8407 and 8050) have $\delta^{18}O$ from –7.2 to –7.5‰. And bores on the east side (WWD8023, 8428, 8429, 8391 and 8089) have $\delta^{18}O$ of –6.9 to –7.1‰. Bore 8110 (501 m depth) has a value matching those of the deep bores 8407 and 8050. Bore 8407 has shown no change in $\delta^{18}O$ from 1988 to 2002.

These results indicate that the ground waters are from at least two sources; shallow waters with $\delta^{18}O$ in the range –6.7 to –7.1‰, which are as expected for present-day rainfall, and deeper waters with more negative $\delta^{18}O$ values (–7.2 to –7.5‰). (Elevation of about 600 m would be required to

produce $\delta^{18}O$ values of –7.5‰.) This relationship is shown in Figure 2.2; deeper bores are found to have more negative $\delta^{18}O$ values than shallow bores. This might suggest that the water at depth is recharged at higher altitude than the shallow water, except that the shallow water has $\delta^{18}O$ values matching what is expected for present-day rainfall including rainfall on the Rosedale Hills. This means that the deep waters cannot easily be accounted for by precipitation at higher elevation.

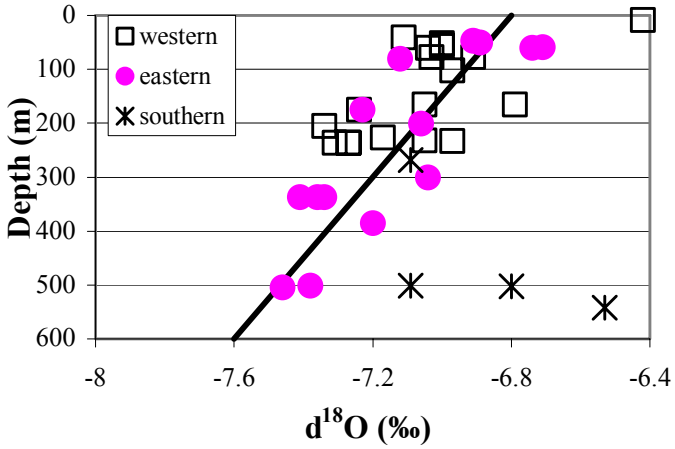

Figure 2.2: $\delta^{18}O$ values versus bore depths. A line is fitted to the points and connects deep (-7.6‰, 600m) and shallow (-6.8‰, 0m) end-members. (Three southern zone points are excluded from the correlation.)

Hence, the favoured explanation is that there are two types of water in the Moutere aquifers. The first is a body of 'fossil' water occupying deeper levels of the Moutere aquifers, which has lower $\delta^{18}O$ values because it was recharged during the last glacial period (in the Pleistocene). Above this is 'modern' water, probably recharged in the last few hundred years of the Holocene, with $\delta^{18}O$ values much the same as today. These two end member compositions are shown by the hollow squares in Figure 2.2; the line connecting them shows the effect of mixing of these waters. Many of the deeper bores are thought to be drawing on both types of water, because they are open for most of their depths. The ^{14}C results support the glacial age of the deep water (see below). (Older Holocene water may also be present in the modern component.)

In the southern zone of the valley, the $\delta^{18}O$ values are more scattered. Bore 8360 is close to the Rosedale Hills, its $\delta^{18}O$ is –7.15‰ (a value expected for local recharge). Also similar are 8107 and 8402 at –7.09 and –7.14‰. Although bore 8029 is deep, the water comes from relatively shallow depth because it contains a trace of tritium. Its $\delta^{18}O$ is –6.53‰. Bore 8109 has an unusually negative $\delta^{18}O$ (–8.28‰), almost certainly indicating glacial age water. Bores 8054 and 8108 have values more typical of present rainfall (–7.09 and –6.80‰). These bores do not draw on a consistent deep component like the deep bores in the western and eastern zones.

Carbon Isotope Compositions

Carbon-14 is the major tool for dating old groundwater. ^{14}C (half-life 5730 years) is generated by cosmic rays in the atmosphere and introduced into living biomass by photosynthesis, and into the hydrosphere by CO_2 exchange reactions. Consequently, any carbon compound derived from atmospheric CO_2 since the late Pleistocene can potentially be dated by ^{14}C.

^{14}C concentration or activity (a) is expressed as percent modern carbon (pmC), where the activity of "modern carbon" is taken as 95% of the activity in 1950 of the NBS oxalic acid standard. Groundwater dating by ^{14}C is complicated by changes in ^{14}C activity in the atmosphere during the late Pleistocene and Holocene, and by dilution of ^{14}C in groundwater by dead carbon derived from soils and rocks when carbon-bearing solutions penetrate underground.

Most of the ^{14}C in groundwater is gained from the soil, where CO_2 accumulates by root respiration and decay of vegetation. The ^{14}C in dissolved inorganic carbon (DIC) is susceptible to reaction and dilution with dead carbon from carbonate, other minerals and organic matter in the soil and groundwater zones. A dilution factor q is used to take account of the resulting dilution of ^{14}C. The age equation is written

$$t = (1/\lambda) \cdot \ln (q \cdot a_o / a_t) \qquad (4)$$

where a_o is the initial ^{14}C activity ($q.a_o$ the diluted initial activity in the groundwater), a_t is the ^{14}C activity in groundwater after time t (i.e. when measured) and λ is the carbon-14 decay constant ($1/\lambda = T_{½} / \ln 2 = 8267$ years). The apparent simplicity of this equation is deceptive. Numerous methods have been proposed for estimating q, based on the chemical and ^{13}C composition of the groundwater.

The carbon-13 concentrations in dissolved inorganic carbon (DIC) from Moutere are shown in Figure 2.3a (plotted against 1/bicarbonate). The $\delta^{13}C$ values are remarkably uniform around the values –20 to -24‰ (except for one sample, see below). This range shows that all of the carbon is sourced from organic matter within the soil or aquifers (Clark and Fritz, 1997). Waters gain dissolved CO_2 by plant respiration and oxidation of organic matter as they pass through the soil, where CO_2 partial pressures are commonly 10 to 100 times those in the atmosphere. The second source is from carbonaceous matter within the aquifers, in this case from the intervening clay layers between the aquifers. Oxidation of such matter produces CO_2 if chemical and/or microbiological conditions are suitable (bacteria are needed to catalyse redox reactions between water and organic matter).

a)

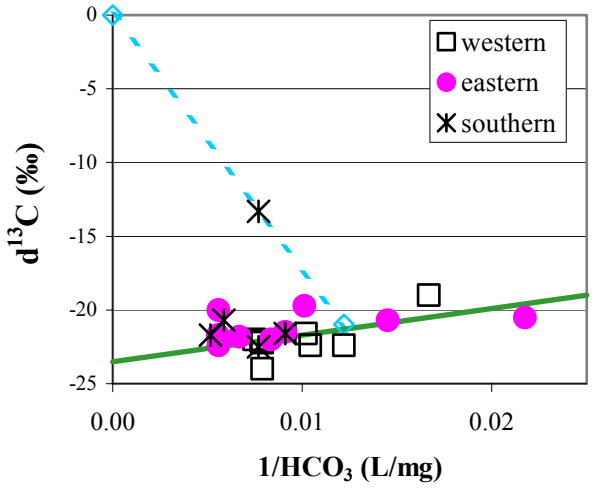

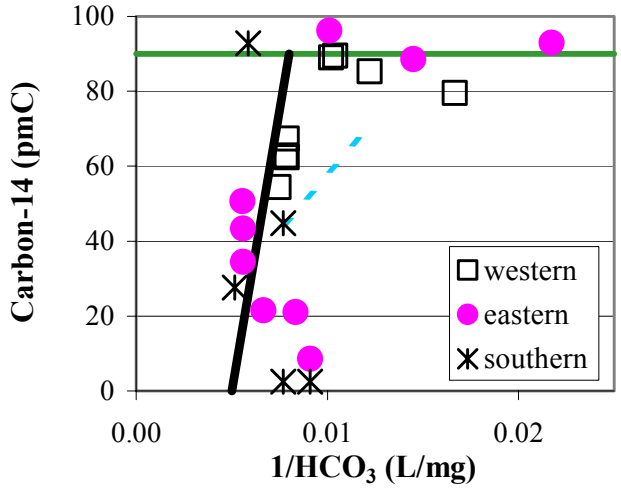

b)

Figure 2.3: (a) $\delta^{13}C$ values versus $(HCO_3)^{-1}$ for bore waters. All except one southern zone water have $\delta^{13}C$ of –20 to -24‰ showing that the carbon is derived from organic matter. (b) ^{14}C values versus $(HCO_3)^{-1}$ for bore waters. The line connects the old (zero ^{14}C, 200 mg/L bicarbonate) and young (90 pmC ^{14}C, 125 mg/L bicarbonate) end-members. Addition of modern plant carbon within the soil moves the points to the left along the line at 90 pmC.

Dissolved CO_2 tends to react with soil and aquifer minerals, acting as the main chemical weathering agent. However, many of these waters have had only limited chemical reaction with the aquifer rocks, because they still contain considerable amounts of dissolved CO_2. This is partly because of the unavailability of carbonate minerals, but weathering reactions with silicate minerals such as albite and anorthite also neutralise dissolved CO_2, e.g.,

$$NaAlSiO_3 + CO_2 + 5.5H_2O > Na^+ + 0.5Al_2Si_2O_5(OH)_4 + 2H_4SiO_4^o + HCO_3^-$$

$$CaAl_2Si_2O_8 + 2CO_2 + 3H_2O > Ca^+ + Al_2Si_2O_5(OH)_4 + 2HCO_3^-$$

However, these reactions are slow. The line through the points in Figure 2.3a traces the evolution of water, which gains bicarbonate by solution of CO_2 and reaction with rock, as it goes underground.

Only one sample has $\delta^{13}C$ outside the range –20 to -24‰, namely WWD8107 with $\delta^{13}C$ of –13.3‰. This sample is likely to have reacted with marine carbonate, which has the effect of moving the sample towards the $\delta^{13}C$ value of such carbonate (approximately 0‰). The dashed blue line in Fig. 2.3a shows the effect of reaction with marine carbonate. Carbon from carbonate rock would have zero ^{14}C, hence it would have a diluting effect on the ^{14}C concentration. The short blue (dashed) line in Fig. 2.3b shows the effect of reaction with carbonate on this sample.

Figure 2.3b shows ^{14}C concentrations plotted against $1/HCO_3$. The ^{14}C concentrations show a wide range of values, from almost 0 to 100 pmC. Shallow bores have ^{14}C concentrations in the range 90 ± 10 pmC. These values are a little less than 100 pmC, because plant material within or below the soil is likely to have ^{14}C concentrations less than modern (~100 pmC) if soils contain material older than a few hundred years. (None of the waters have concentrations high enough to indicate the presence of carbon-14 from nuclear weapons testing and hence are ‘pre-bomb’; i.e. they were all recharged before the early 1960s.) The line at 90 pmC in Fig. 2.2b shows the effect of increasing bicarbonate concentration by solution of CO_2 and reaction with rock within the soil. Points along

this line (from right to left) trace the evolution of the modern water component as it goes underground (in the same process as illustrated for evolution of $\delta^{13}C$ in Figure 2.3a).

The glacial water component has zero ^{14}C. Its bicarbonate concentration is about 200 mg/L. Figure 2.3b shows the mixing line between the glacial and modern end members (shown by squares). The modern water end member involved in the mixing process has bicarbonate concentration of about 125 mg/L.

The ^{14}C concentrations are plotted against $\delta^{18}O$ in Figure 2.4. An approximately linear relationship is seen between them for the western and eastern zone samples, showing mixing between the glacial (with composition -7.6‰, 0 pmC) and modern (-6.8‰, 90 pmC) components (again shown by squares).

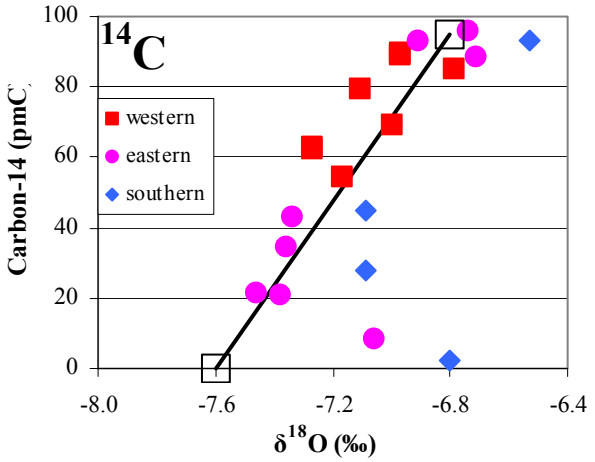

Figure 2.4: $\delta^{18}O$ versus ^{14}C for bore waters; the older waters (low ^{14}C) have more negative $\delta^{18}O$ values.

The areal variations of the ^{14}C concentrations are significant (Figure 2.1c). In the western zone, ^{14}C was measured in one bore (8074) in the recharge zone. This along with WWD8419, 8097 and 8800 has modern (but pre-bomb) ^{14}C concentrations of 90 ± 10 pmC. 8223 also contains a small amount of tritium although its ^{14}C is relatively low (69 pmC). Two of the remaining three wells in the western zone (8007 and 8404) have ^{14}C measurements, the results are 54 and 64 pmC.

In the eastern zone, bores 8343 and 8355 have ^{14}C of 96 and 89 pmC (indicating modern carbon). The deep bores 8407 and 8050 have 43 and 22 pmC respectively. The shallow bore east of the valley floor (8429) has modern carbon (93 pmC), while the deep bores (8110 and 8089) are quite old with 21 and 9 pmC respectively.

In the southern zone, 8029 has modern carbon (93 pmC), 8107 and 8054 have 45 and 28 pmC, and 8108 and 8109 are very old with only 2.4 pmC. Hence there are glacial age waters in the southern zone, but there is not the consistent pattern with $\delta^{18}O$ that is found in the western and eastern zones.

Chemical Compositions

The chemical compositions of the western and eastern zone waters are affected by mixing of the two water types. The glacial water at depth appears to have a nearly uniform composition, whereas the modern water penetrating from the top has a more varied composition.

Chloride concentrations in groundwater often reflect marine influence on rainfall (i.e. rainout of seasalt particles in the atmosphere). For rainfall recharged groundwater, evapotranspiration

causes enrichment of chloride while passing through the soil. A third influence is sea water trapped within deep parts of the aquifer during past higher sea level stands, or present-day intrusion of sea water. The plot of chloride versus $\delta^{18}O$ (Figure 2.5a) shows glacial water (Cl ~ 5.5 mg/L, $\delta^{18}O$ ~ -7.6‰) mixing with modern water containing a range of chloride values (5.5. to 18 mg/L, $\delta^{18}O$ ~ -6.8‰). The graph has two limbs. Most of the western and eastern bores have chloride near 5.5 mg/L. However, bores on the seaward side of the Moutere Valley (WWD8110, 8423, 8391 and 8089) plot on the upper limb with higher chloride concentrations. This is considered to reflect their location nearer the sea where they receive rainfall that has higher chloride concentrations. If so, this shows that the recharge occurred locally. Wells WWD8050, 8007 and 8419 (1988 sample) have markedly higher chloride concentrations because of input of sea water (these points are not plotted in Figure 2.5a).

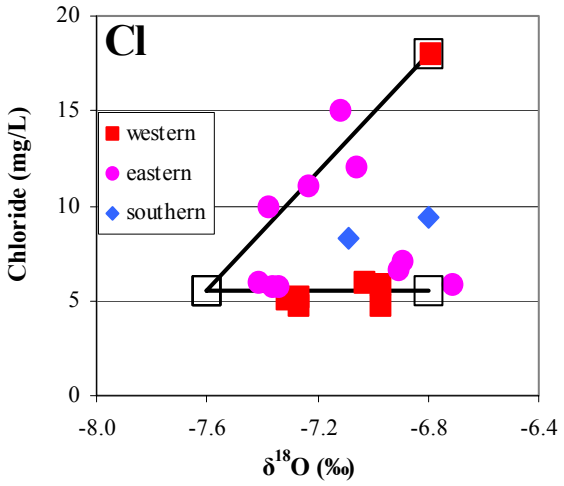

a)

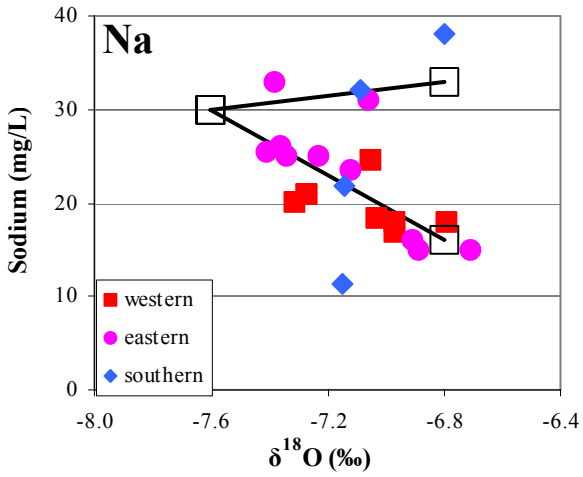

b)

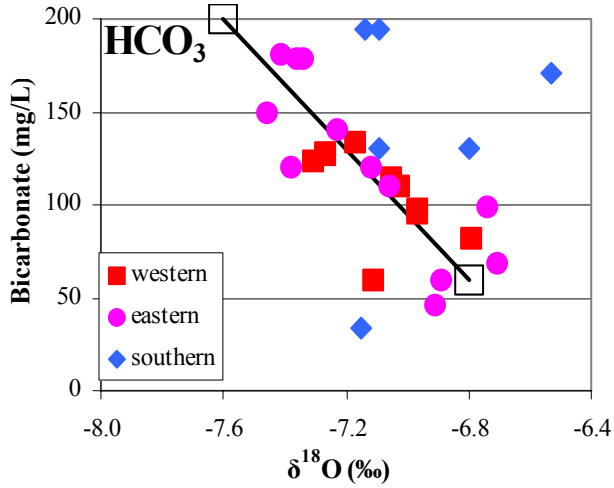
HCO3
Bicarbonate (mg/L)
200
150
100
50
0
western
eastern
southern
-8.0
-7.6
-7.2
-6.8
-6.4
δ18O (‰)

c)

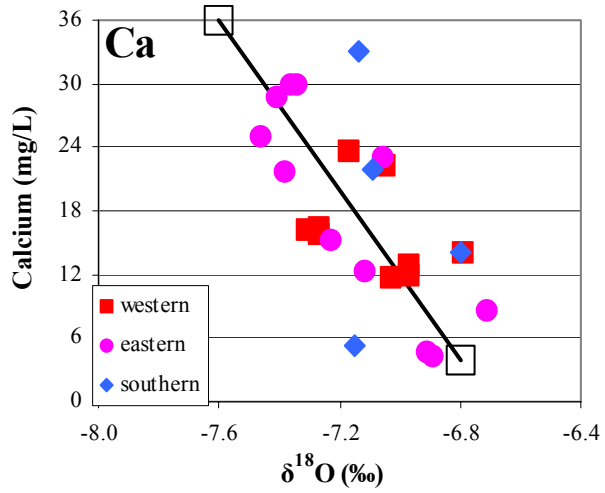
Ca
Calcium (mg/L)
36
30
24
18
12
6
0
western
eastern
southern
-8.0
-7.6
-7.2
-6.8
-6.4
δ18O (‰)

d)

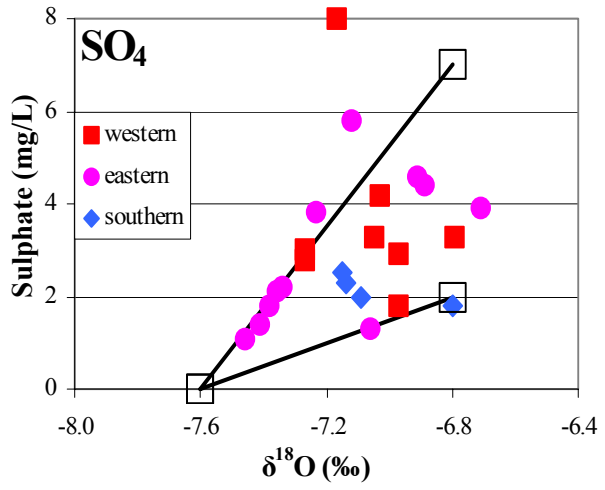
SO4
Sulphate (mg/L)
8
6
4
2
0
western
eastern
southern
-8.0
-7.6
-7.2
-6.8
-6.4
δ18O (‰)

e)

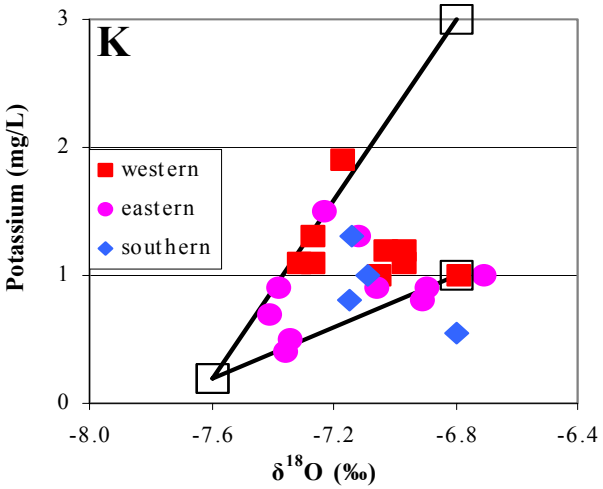
K
western
eastern
southern
Potassium (mg/L)
δ18O (‰)
3
2
1
0
-8.0
-7.6
-7.2
-6.8
-6.4

f)

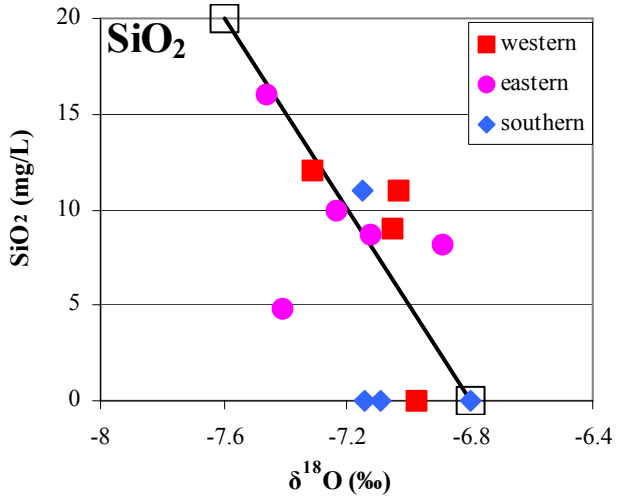
SiO2
western
eastern
southern
SiO2 (mg/L)
δ18O (‰)
20
15
10
5
0
-8
-7.6
-7.2
-6.8
-6.4

g)

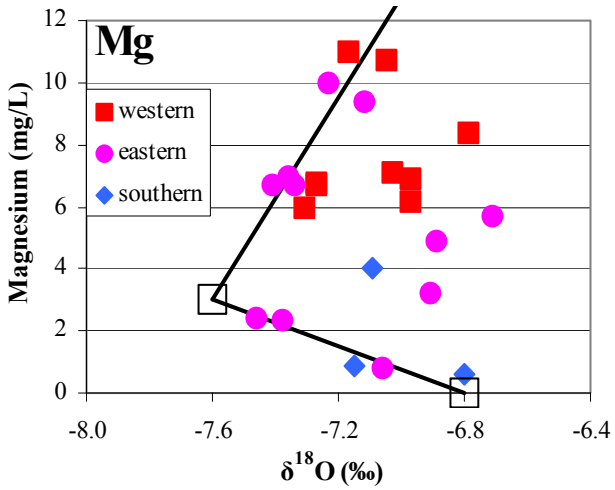
Mg
western
eastern
southern
Magnesium (mg/L)
δ18O (‰)
12
10
8
6
4
2
0
-8.0
-7.6
-7.2
-6.8
-6.4

h)

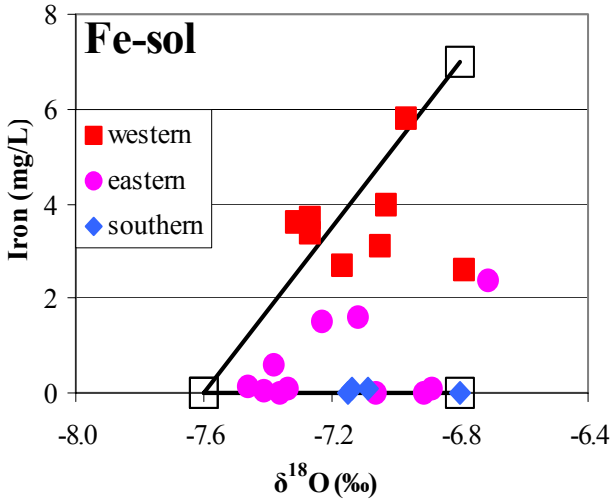

i)

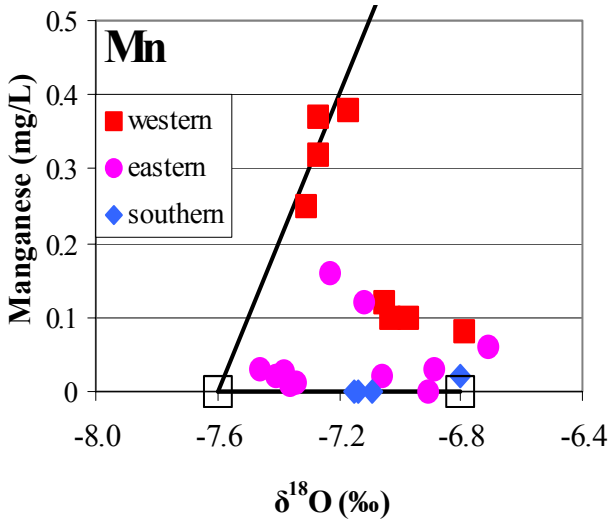

j)

Figure 2.5 (a-j): $\delta^{18}O$ versus Cl, Na, HCO_3, Ca, SO_4, K, SiO_2, Mg, soluble Fe and Mn concentrations. Lines connect end-members at $\delta^{18}O$ values of –7.6‰ (glacial water) and –6.8‰ (modern water).

Sodium (Figure 2.5b) has similarities to chloride, but is more affected by interaction with aquifer rocks. Sea water influence is shown by higher sodium concentrations in WWD8050 and 8007 (not plotted). The plot with $\delta^{18}O$ shows two limbs as with chloride, but the upper limb values are more scattered (although it still includes two of the same bores, i.e. 8110 and 8089). Most of the samples lie on the lower limb, forming a trend towards higher sodium at depth because of increased water/rock interaction.

Bicarbonate and calcium (Figures 2.5c and d) are readily affected by reaction with soil and rock, and the deep component has higher concentrations of these constituents than the shallow component. This is consistent with greater interaction with rock with depth (i.e. residence time).

Sulphate and potassium (Figures 2.5e and f) are lower in the deep component compared to the shallow component. For sulphate, this is because of chemical reduction in anaerobic environments affecting the deep component. Potassium (like sodium) is affected by interaction with rock, but the rock tends to take up potassium instead of releasing it.

Silica and magnesium (Figure 2.5g and h) show considerable scatter related to rock/water interaction. For silica, there appears to be a trend towards higher silica with depth, but some high values of silica are not plotted. Magnesium shows relatively uniform concentrations in the deep water, but widely varying concentrations in the shallow component. The western (and some eastern) zone bores have the higher magnesium concentrations.

Soluble iron and manganese (Figures 2.5i and j) show widely varying concentrations. Western zone bores have higher concentrations, while a number of eastern bores have very low concentrations. The deep component has a low concentration. Soluble iron and manganese are affected by the redox conditions of the waters.

The compositions of the end-member waters have been determined from the mixing plots (raw values are in Stewart, 2002; Table 4).

Tritium and CFCs

Tritium and CFCs can be used to determine the ages of waters too young to be dated by ^{14}C. The minimum age that can be determined by ^{14}C is about a thousand years, unless bomb ^{14}C is present. Tritium and CFCs can give ages in the range of zero to some hundreds of years. The histories of the concentrations of tritium and CFCs in the atmosphere are shown in Figure 2.6 (Stewart and Morgenstern, 2001). Tritium concentrations passed through a peak in the 1960s and 1970s because of tritium produced by atmospheric nuclear weapons tests. Since then tritium concentrations have declined, reaching the cosmic ray-produced background level of about 2 TU around 1985. Tritium has a radioactive half-life of 12.32 years. CFC-11 and CFC-12 are entirely anthropogenetic in origin and their concentrations in the atmosphere rose from zero in about 1940 to peak in the 1990s. CFC-11 concentration has slowly declined since about 1993, while CFC-12 concentration is still increasing but at a much slower rate than before 1990.

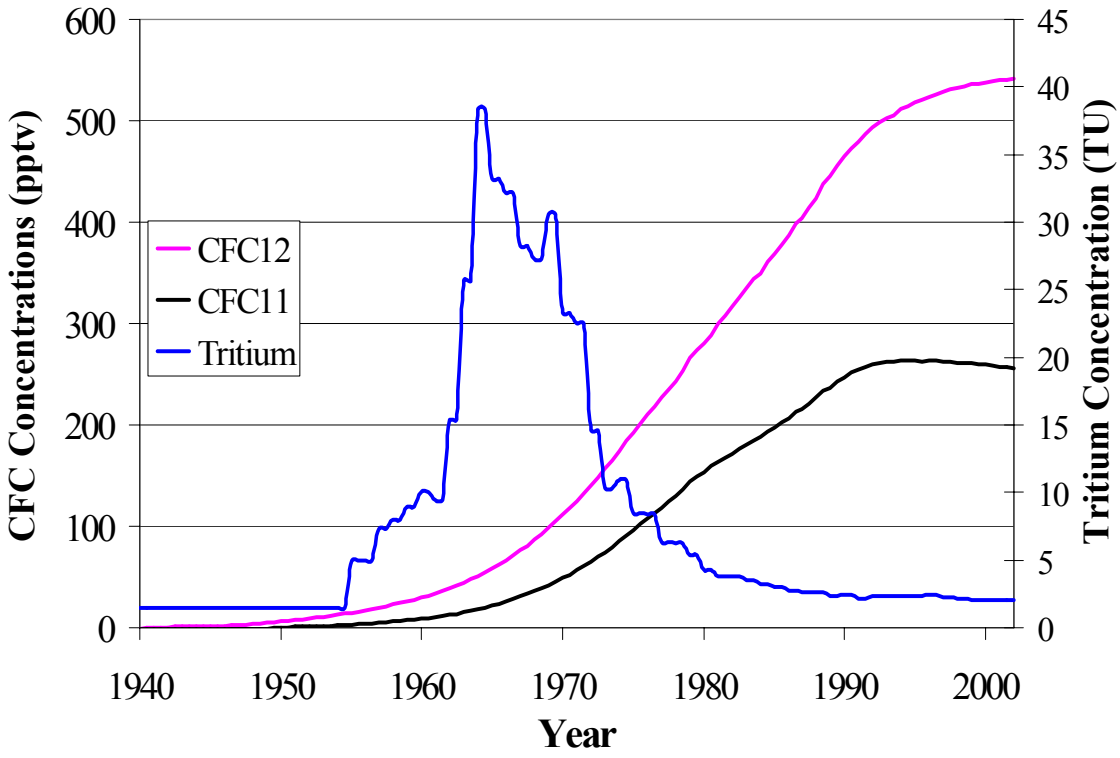

Figure 2.6: History of tritium concentration in precipitation at Kaitoke (near Wellington) and CFC concentrations in the Southern Hemisphere atmosphere.

Tritium samples were collected from Moutere Valley bores in 1984-1988 and 1998-2002. All but one of the 1984-1988 results had concentrations that were too low to measure (Thomas, 1989,

1992); i.e. their concentrations were zero within the accuracy of measurement. These show that not only were the waters old on average, but that both water components (modern and glacial) are old on the timescale of tritium. The samples contain about 50% of the glacial and 50% of the modern water components (from ^{18}O and ^{14}C results). The glacial component will have zero tritium, therefore the maximum the modern component can have is 0.48 TU. (This is twice the measurement error of ±0.12 TU divided by 50%.) This gives a minimum age of 90 years for the modern component assuming a mixing model with a relatively wide distribution of residence times (namely a dispersion model with a dispersion parameter (DP) of 0.2, which is equivalent to an exponential piston-flow model with 63% mixing,). The only sample of this group which contained tritium (WWD8360), came from a shallow bore on the Rosedale Hills. Its value of 1.21 TU showed influence of bomb tritium and a mean residence time of 57 years for the same mixing model as before (DP = 0.2, 63% mixing).

Measurements during 1998-2002 had smaller measurement errors (±0.02 TU for low tritium concentrations). A number of samples (WWD8404, 8800, 8012, 8050, 8355, 8054) had tritium concentrations below the detection limit; for these the modern component has less than 0.08 TU tritium assuming 50:50 modern/glacial mixtures. The minimum mean age for these is 150 years (for DP = 0.2, 75% mixing).

Bore WWD8407 unexpectedly showed a trace of tritium. The 1988 sample had 0.13 ± 0.05 TU and the 1999 sample 0.050 ± 0.016 TU. Assuming a 30:70 modern/glacial mixture, the modern component has 0.17 TU; this gives a minimum mean age of 120 years (DP = 0.2, 72% mixing). It is more probable however that the tritium is brought in at a shallow depth by a very small fraction of much younger water (i.e. with higher tritium concentration).

The shallow bores WWD8223 and 8343, on the west side of the Moutere Valley, contained tritium. 8223 had a trace of tritium with 0.070 ± 0.016 TU and a modern/glacial makeup of between 100/0 and 80/20. Assuming the former, the mean age is 150 years ((DP = 0.2, 75% mixing). Its CFC-11 age was greater than 110 years, in agreement with the tritium age. 8343 had 0.894 ± 0.034 TU giving a mean age of 67 years (DP = 0.2, 55% mixing). Its CFC-11 concentration gave a mean age of 32 years with the same mixing model. The difference (67 and 32 years) shows that the mixing model used must be incorrect. The tritium and CFC-11 ages can be reconciled by using a model with 40% 13 year old water and 60% water old enough to have no tritium or CFC-11. The 40% of younger water shows recent recharge.

Bores WWD8074 and 8085 are in the Waiwhero area. Their tritium concentrations (1.94 ± 0.06 TU, 2.21 ± 0.06 TU) are in the ambiguous range and mean ages could be 13-16 years or 32-37 years (DP = 0.2). However both have CFC measurements with CFC-11 indicating ages of 12-16 years. (CFC-12 ages are younger still at 7-12 years, but the CFC-11 ages are generally preferred.) In either case, the CFCs show that the younger tritium ages are the correct ones.

Bore WWD8029 had a trace of tritium (0.053 ± 0.019 TU) giving a mean residence time of 165 years (DP = 0.2, 76% mixing).

These results show that the deep waters did not contain detectable tritium or CFC concentrations when first measured (as expected) and continue to show none.. And if anything, carbon-14 concentrations appear to be getting lower rather than higher since 1988.) On the other hand, groundwater levels, which are drawn down during the summer, generally recover during the subsequent winter and early spring. Thus recharge is occurring, but this new water must be near the surface in the recharge areas and has not yet found its way to the aquifers tapped by the deep bores or younger water is slowly penetrating but dilution with old water is sufficient to keep concentrations at less than detectable levels.

2.3 Discussion

Nature of the system

The $\delta^{18}O$ values of the western and eastern zone groundwaters show a linear relationship with depth (Figure 2.2). This indicates the presence of two types of water, because the $\delta^{18}O$ values are not likely to change underground. Consideration of the likely mean $\delta^{18}O$ of rainfall in the Moutere Valley indicates that the shallow groundwater derives from present-day rainfall (around –6.8‰). Even water recharged at the highest altitudes in the Rosedale Hills (250-300 masl) would not have $\delta^{18}O$ values as negative as the deep water (-7.6‰).

The ^{14}C concentrations show a relationship with the $\delta^{18}O$ values (Figure 2.4), hence the shallow waters are young and the deep waters old in terms of ^{14}C. These are the modern and glacial water types identified above. The bores discharge either modern or mixtures of modern and glacial water. None of the western or eastern bores discharge pure glacial water. The glacial water is believed to have been recharged during the last glaciation (20-50,000 years ago).

Glacial water body

This water is deep and very old. During the last glacial maximum, the sea level is believed to have been at least 120 m lower than its present level, and therefore the sea was a long way (100s of kms) from its present position. If the aquifer does not connect to the sea, there is likely to be a very large body of freshwater or mainly freshwater underlying part of Tasman Bay.

This body of water was probably recharged over a considerable period during the last glaciation. A minimum mean age can be estimated using equation 4. We assume that the ^{14}C activity of the deep water is less than 1 pmC, and that of the shallow water is 90 pmC. The bicarbonate concentrations in the deep and shallow waters are 200 and 60 mg/L respectively, hence the dilution factor (q) is 60/200. These give a mean age of greater than 27,000 years.

This water is being drawn on and presumably the part under Moutere Valley will gradually be replenished by younger water. It is probable that there is very little natural flow through the deep aquifer. The lack of ^{14}C indicates that no recharge has taken place into this water body since the last glaciation (i.e. in the Holocene). Some of the water is now being extracted by deep bores, causing marked drawdowns in water levels during the late summer. However, levels recover during the winter. Hence recharge is occurring, and there must be a tendency for shallow water to penetrate deeper as deep water is extracted.

Where repeated measurements have been made (WWD8404 and 8407), there appears to be a trend towards ages becoming older due to exploitation. This suggests that more of the deep water is being extracted because permeabilities at depth allow more efficient recovery (i.e. water flows more rapidly in the deep aquifer).

Shallow water body

The shallow water body is modern or pre-industrial Holocene water, and recharge has occurred before the advent of carbon-14 and tritium from nuclear weapons testing (i.e. the 1960s) for the bores sampled. The ages are mostly in the hundreds of years. Recharge appears to have been relatively widespread, albeit at a very low rate. The evidence (including $\delta^{18}O$ values and chloride concentrations) suggests that rainfall has infiltrated into the hills both east and west of the Moutere Valley floor (i.e. into both the tm1 and tm2 outcrop units of Moutere Gravel) in the past.

Only sporadic traces of tritium and CFCs have been observed, and these are generally in shallow bores on the western hills and western side of the Moutere Valley floor. Tritium was observed in WWD8074 and 8085 in the Waiwhero area, and in 8223 and 8315 on the west side of the valley floor west of the fault. WWD8343 and 8407 (trace only) are the only eastern zone bores to contain tritium. Tritium was detected in the shallow bore on the Rosedale Hills (WWD8360) and in 8029 (trace) in the southern zone. CFC occurrences are consistent with the tritium detections. Hence in summary, the highest tritium concentrations are found in shallow groundwater in the hills west of

the valley floor. This suggests that the most active recharge is in this region and very probably into the tm1 outcrop area (Thomas 1992, Figure 1.1). However, there is no direct geochemical evidence for the latter, because no such young water has yet reached bores tapping the Deep or Middle Moutere Aquifers.

A revised pattern of recharge and groundwater flow for the Moutere Aquifers is given in Figure 2.7 in light of this work. Rainfall recharge into the hills both west and east of the Moutere Valley is shown. (There could also be a recharge contribution from Waiwhero Stream on the west side.) But under the natural situation, this recharge is believed to be flowing at shallow or intermediate levels, leaving an undisturbed body of ice age water at deep levels. This pattern results from the present sea level and the expected lack of offshore outlets for water in the deep aquifer. Groundwater exploitation from deep bores will now be tending to draw shallow water deeper into the system.

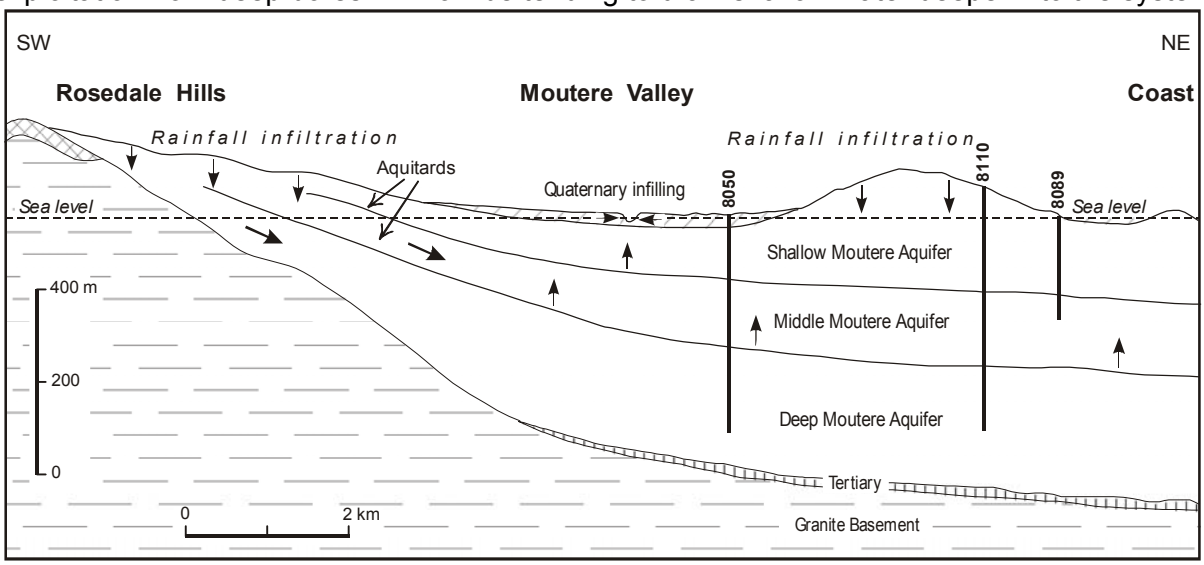

Figure 2.7: Revised recharge patterns for the Moutere aquifers in light of this work.

2.4 Conclusions

Recharge to the Moutere Gravel aquifer system in the Moutere Valley was investigated by means of isotopic and chemical measurements. Bores up to 500 m deep tap three Moutere Gravel aquifers underlying the area. Shallow bores (50-100 m) have $\delta^{18}O$ in the range –6.8 ± 0.4‰ expected for present-day rainfall. Their carbon-14 concentrations are generally 90 ± 10 pmC indicating modern ages, i.e. water residence times of up to hundreds of years.

Deeper bores have more negative $\delta^{18}O$ values and lower ^{14}C concentrations resulting from input of much older water from depth in the western and eastern zones. The old deep water is believed to have been recharged in the Pleistocene during the last glaciation. This 'glacial' water has $\delta^{18}O$ of –7.6‰, and ^{14}C concentration of 0 pmC. Mixing of glacial and modern waters gives rise to the variations observed in the oxygen-18, carbon-14 and chemical concentrations in the bore waters. The chemical characteristics of the glacial water have been determined as end members on mixing plots between chemical components and $\delta^{18}O$. Sea level was much lower when the glacial water was recharged, and the sea would have been far from its present position. A large body of glacial water may be resident in the Moutere Gravel under Tasman Bay.

Recharge is provided by modern water penetrating the groundwater system at shallow levels. Measurements on this water give evidence on the patterns and rates of recharge. The distribution of $\delta^{18}O$ and chloride suggest that water has been recharged through both the tm1 and tm2 units of Moutere Gravel in the past few hundred years, but evidently at very low rates because of the ages.

Young recharge is observed only on the hills west of the valley floor, but observations are lacking in the most probable recharge zone (the tm1 outcrop area in the Rosedale Hills).

CHAPTER 3: NEUROFUZZY MODELLING OF GROUNDWATER ABSTRACTION

3.1 Study Objective

Recently, concerns over adverse impacts of groundwater abstraction operation on groundwater system in Moutere Western Groundwater Zone have led to a reevaluation of the abstraction.

In order to evaluate the effect of groundwater abstraction on groundwater system dynamics in Moutere catchment, a hybrid dynamic neurofuzzy model system (Hong et al. 2002), integrating a fuzzy rule-based model and an artificial neural network, is developed to predict the change of groundwater levels due to the operation of abstraction in Moutere Western Groundwater Zone in 1994 and 2001. The dynamic neurofuzzy model is calibrated using observed groundwater level at Palmers (site No.: 1219435), rainfall at Kellings Road (site No.: 132010), and actual abstraction data in the period 1994-11-07 to 2001-06-18. The operation of abstraction with five different scenarios are then used to predict the change of groundwater levels at Palmers affected by different abstraction scenarios and the predictions are compared with observations of actual historical groundwater levels at Palmers in 1994 and 2001.

The modelling procedures used to address the objective are:

1. Develop a dynamic neurofuzzy model to predict the effects of an actual historical abstraction take on the groundwater levels at Palmers in the period 1994-11-07 to 2001-06-18.
2. Run the calibrated dynamic neurofuzzy model with five different weekly synthesised abstraction scenarios to predict the groundwater levels at Palmers.
3. Investigate the effects of different weekly synthesised abstraction scenarios, especially in a dry season (1997 and 2001 years), on groundwater levels at Palmers. Calculate summary statistics and assess any differences.

3.2 Methodology – Dynamic neurofuzzy System

In this section, the basis of the dynamic neurofuzzy system (DNFS) are described.

Fuzzy sets

A fuzzy system is used to represent the imprecision found in natural language. To describe this, Zadeh (1973) introduced the concept of a fuzzy set. Fuzzy sets represent vague description of objects i.e. tall, small, cold, bright, etc.

For conventional sets, rigid membership requirements are imposed upon the objects within the set. An object is a member of a set to degree 0 (not in the set at all) or 1 (completely in the set). For example, the set of TALL men could be defined to be all men 6 feet or taller (Fig. 3.1). As shown in Fig. 3.1, the conventional set classifies a man as either TALL, or not TAL. There is no middle ground. In contrast, fuzzy sets have more flexible membership requirements that allow for partial membership in a set. A man 6 feet tall is a member the fuzzy set TALL to degree 0.5 (Fig. 3.1). A man 5 feet 6 inches tall is TALL to degree 0.25, a man 6 feet 6 inches tall is TALL to degree 0.75.

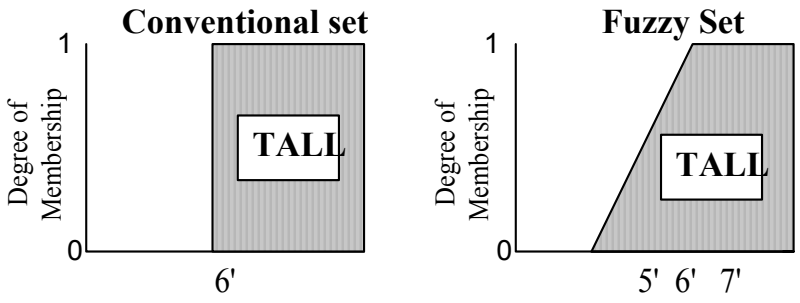

Figure 3.1: Conventional Sets vs. Fuzzy Sets.

Mathematically, a fuzzy set, A, is a function defined on the universe of discourse, *X*, given by:

$$u_A(x): X \rightarrow [0,1] \quad (1)$$

where A is the linguistic variable (or fuzzy label) describing the variable *x*. The universe of discourse of a variable is its range and can be either continuous or discrete. $u_A(x)$ represents the membership function, *x* belonging to the fuzzy set A. In general, the shape of a membership function depend on the application and can be trapezoidal, bell-shaped, triangular, or Gaussian, etc as shown in Fig. 3.2.

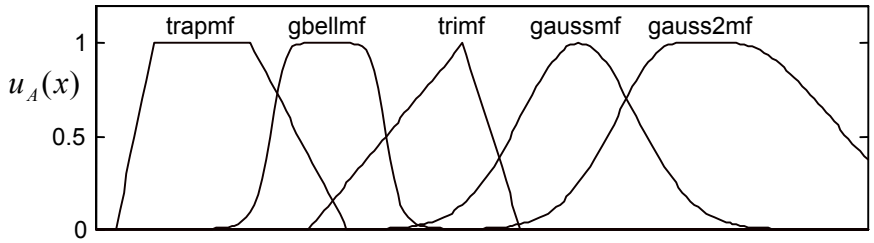

Figure 3.2: Different shapes of fuzzy membership functions.

Figure 3.3 illustrates one example of the discourse for the linguistic variable temperature. Linguistic values, which define these variables, are: Cold, Warm, and Hot.

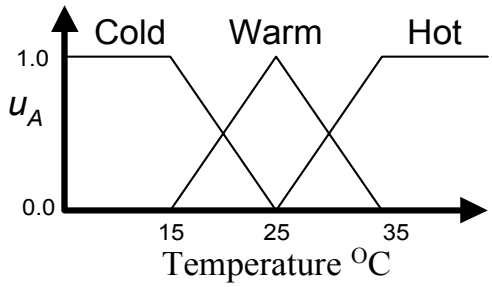

Figure 3.3: Typical fuzzy set for temperature.

Fuzzy inference system

To construct a fuzzy system we have to describe mapping from one universe of discourse to another and this can be achieved using fuzzy algorithms. Fuzzy IF-THEN rules (or fuzzy *implication* statements) can be used to describe part of such a mapping and a collection of rules from an algorithms. Depending on the encoding method of a fuzzy algorithm, several fuzzy-rules-

base systems can be distinguished: linguistic fuzzy model (Mamdani, 1974), fuzzy relational model (Pedrycz, 1983), Takagi-Sugeno model (Takagi & Sugeno, 1985).

In fuzzy inference system (or fuzzy-rules-base system), every fuzzy rule has a two parts:

antecedent part(premise), expressed by: *IF*…
consequent part, expressed by: *THEN*…

The antecedent part is the description of the state of the system which should turn on the rule, and the consequent is the action that the operator who controls the system must take. Consider the following example of dealing with a problem of a high groundwater level affected by abstraction based on linguistic fuzzy model:

$$\text{IF } \overbrace{(\text{Rain is High}) \text{ AND } (\text{Abstraction is Low})}^{\text{antecedent}} \text{ THEN } \overbrace{(\text{GW L is High})}^{\text{consequence}} \qquad (2)$$

where: Rain is rainfall,
Abstraction is groundwater abstraction rate,
and GWL is groundwater level.

In this example, Rain, Abstraction, and GWL are linguistic variables, and Large, High, and very High are linguistic values (or fuzzy labels) that are characterised by appropriate membership functions. The linguistic values 'Large', 'High', and 'Very High' have a certain degree of vagueness and fuzziness. This fuzziness can be described by membership functions which can assume different curves, e.g. straight lines, triangular, bell-shaped, Gaussian, and so forth (Fig. 3.2).

Every fuzzy inference system (or fuzzy controller) is composed of four principal blocks as shown Fig. 3.4 (Jang, 1993):

knowledge base (rules and parameters for membership functions),
decision unit (inference operations on the rules), fuzzification interface (transformation of the crisp inputs into degrees of match with linguistic variables), and
defuzzification interface (transformation of the fuzzy results of the inference into a crisp output).

In many engineering applications, the inputs and outputs are numerical values, rather than fuzzy sets. To deal with this, the fuzzy system must be equipped with conversion interfaces, so-called *fuzzification* and *defuzzification* units, as shown in Fig. 3.4.

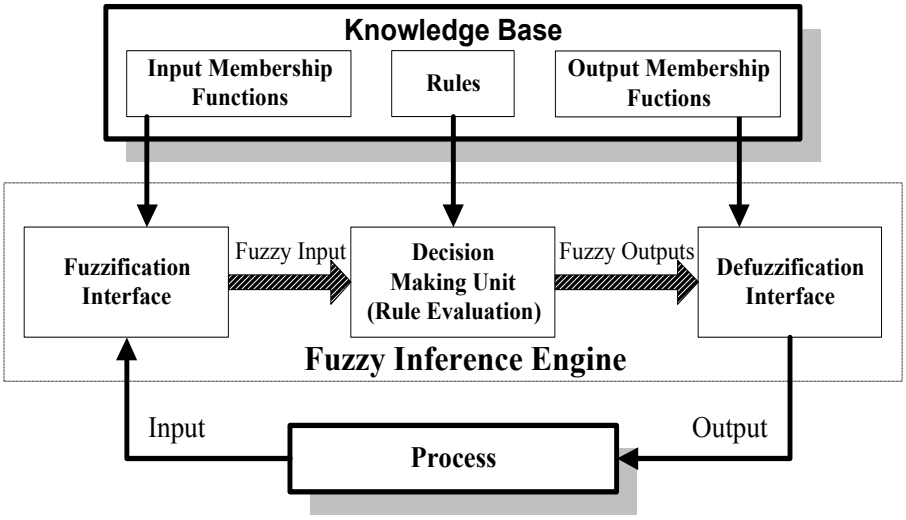

Figure 3.4: General structure of fuzzy inference system.

The fuzzy inference engine of the system from Fig. 3.4 is represented on the Figure 3.5.

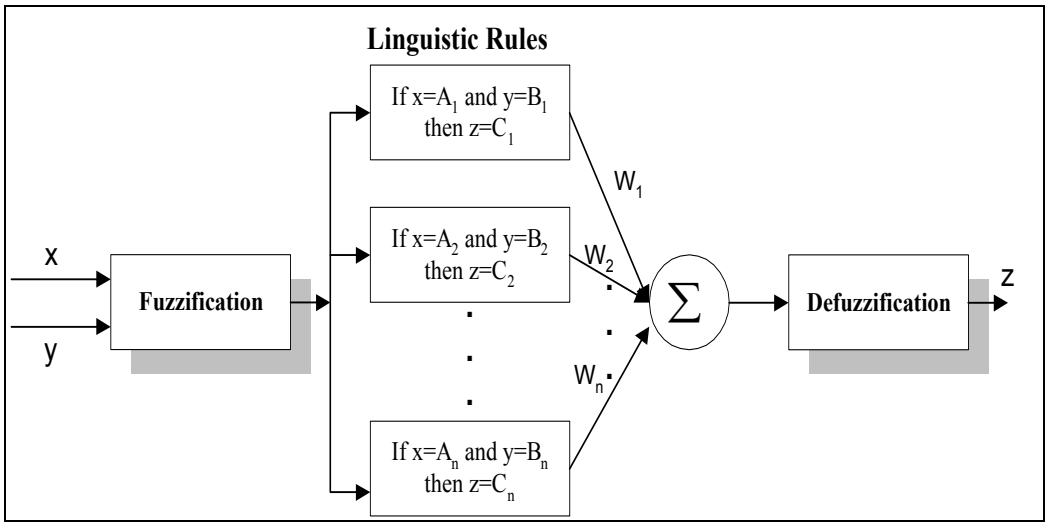

Figure 3.5: General structure of fuzzy inference engine.

In the *fuzzification* unit, input values are considered as fuzzy singletons and membership grades of all fuzzy propositions in the rule antecedents are evaluated. Fuzzification means using the membership functions of linguistic variables to compute each term's degree of validity at a specific point of the process. When a fuzzy rule activates, it fires to a certain degree of depending on the belief level in each antecedents are evaluated in the premise of the rule.

The antecedents are evaluated using membership functions to belief levels, which are then combined using a fuzzy operator (ex. T-norm and T-conorm) to produce the final output activation level. Finally, the output activation level is used to either scale or clip the fuzzy output set. Clipping the output is called Max-Min inference, and scaling the output is called Max-Dot inference. There are a number of fuzzy inference engines, but the most cited in the literature (Jang, 1993) are:

Max-Dot method (type 1). The final output membership function for each output is the union of the fuzzy sets assigned to that output in a conclusion after scaling their degree of membership values to peak at the degree of membership for the corresponding premise (modulation by clipping)

Max-Min method (type 2). The final output membership function is the union of the fuzzy sets assigned to that output in a conclusion after cutting their degree of membership values at the degree of the corresponding premise (linear modulation). The crisp value of output is, most usually, the centre of gravity of resulting fuzzy set
Takagi and Sugeno's method (type 3). Each rule's output is a linear combination of input variables. The crisp output is the weighted average of each rule's output .

In this project, the Takagi and Sugeno inference engine (Takagi & Sugeno, 1985) is used to develop the dynamic neurofuzzy system. This method has generated better prediction result compared to other two engines in many real engineering applications.

Takagi & Sugeno (TS) Fuzzy Model

Takagi and Sugeno (1985) developed a hybrid modelling technique designed to combine conventional and fuzzy modelling. The resulting model, called a TS model is represented by a series of fuzzy rules of the form:

$$\text{IF } (X \text{ is } A^i) \quad \text{THEN} \quad (y = f_i(x_i)) \qquad (3)$$

where $f_i(x_i)$, defined on $x_i \subset X$, is a local model used to approximate the response of the system in the region of the input space represented by the antecedent. The function $f_i(x_i)$ are often chosen as affine linear forms $y_i = a_i^T x + b_i$, where a_i is a parameter vector b_i is a scalar offset.

The overall output of TS model is calculated as a weighted average of the rule contributions:

$$y = \frac{\sum_{i=1}^{K} u_{A_1}(X) f_i(x_i)}{\sum_{i=1}^{K} u_{A_1}(X)} \qquad (4)$$

Eq. (4) serves to combine numerous simple local models to globally represent a system that may be highly nonlinear. Membership functions define the nature of the contribution of each local model to the global model. This algorithm is very effective as the inference and the defuzzification process is integrated into a single step procedure. The main advantage of the TS fuzzy model described is that it tries to decompose the input space into subspaces and then approximate the complex system in each subspace by a simple linear local model. Each fuzzy rule describes a local linear behaviour of the system associated to the fuzzy input region characterised by the antecedent of the fuzzy rule. For this reason, the TS fuzzy model has been successfully applied to many different complex systems. Figure 3.6 shows an example of a TS fuzzy local modelling with three rules " IF *x* is Θ^i THEN $\hat{y} = \alpha_i x + \beta_i$".

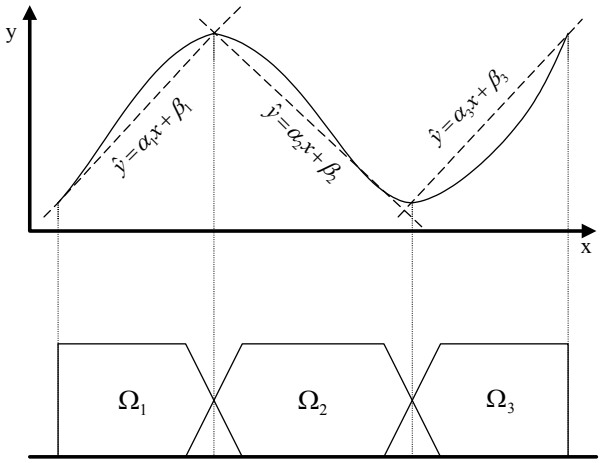

Figure 3.6: Illustration of multiple local models using a TS fuzzy model.

Input space partitioning

Different fuzzy inference systems can have nearly the same antecedents in their fuzzy rules though their consequent constituents are different. There are three major methods of input space partitioning and they are suitable for all types of fuzzy inference systems mentioned in preceding section.

Grid partitioning (Figure 3.7(a))

This method is easy to use and usually is chosen for a fuzzy controller, and in some cases, it can be taken as an initial state of partition for some adaptive partitioning methods. Because the number of rules increases exponentially with the number of inputs, if the tasks have comparative large number of inputs, "the curse of dimensionality" will occur.

Tree partitioning (Figure 3.7(b))
The tree partition can alleviate the problem mentioned above to some extent. In this partition method each region can be uniquely specified along a corresponding decision tree. Usually, it is difficult to express linguistic meanings for the membership functions.

Scatter partitioning (Figure 3.7(c))
The scatter partition has relatively small number of membership functions covering a subset of the input space that characterises a region of possible occurrence of the input vectors. The scatter partition is usually dictated by desired input-output data pairs and generally, orthogonality does not hold. In the dynamic neurofuzzy system (DNFS), we use scatter partitioning.

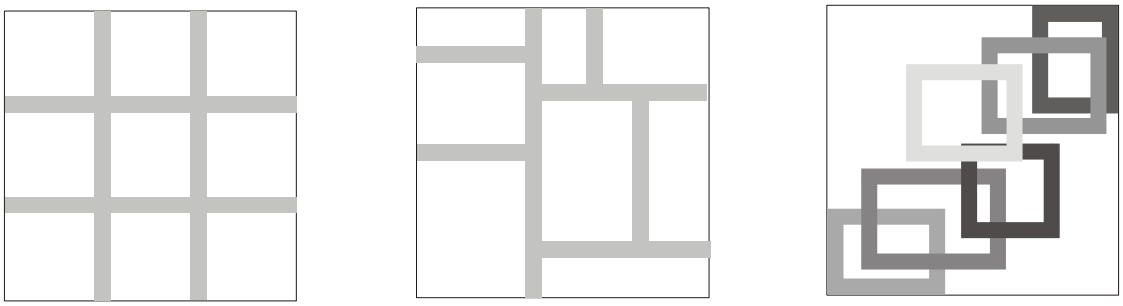

Figure 3.7: Three methods of input space partitioning: (a) grid partition; (b) tree partition; (c) scatter partition.

Dynamic Neurofuzzy System (DFNS)
Fuzzy modelling is a knowledge-based system consisting of linguistic IF-THEN rules that can be constructed using the knowledge of human experts in the given field of interest. Fuzzy modelling also utilises universal approximators that can realise nonlinear mappings. Compared to other nonlinear approximation techniques, fuzzy modelling provides a more transparent representation of the nonlinear systems and appears very useful when the responses to change in manipulated variables are nonlinear or when there is a lack of well-defined mathematical model. However, as system complexity increases, reliable fuzzy rules and membership functions used to describe the systems behaviour are very difficult to determine. Furthermore, due to the dynamic nature of environmental process such as cooling water discharge model, fuzzy rules and membership functions must be adaptive to the changing environment and operating conditions of the power station in order to continue to be useful. The quality of fuzzy modelling can be significantly influenced by changing shapes of membership functions and fuzzy rules. Thus methods for performing the adjustment of membership functions and modification of fuzzy rules are necessary.

In this project, an artificial neural network (ANN) technology is used to compensate the weak points of fuzzy system. This mutual improvement is achieved by combining fuzzy system and ANN, and this new method is called *neurofuzzy* (or *fuzzy neural network*). As shown in Fig. 3.8, the aim of neurofuzzy system is to combine collectively the benefits of both fuzzy system and ANN. The given system is expressed as linguistic fuzzy expressions and learning methods of ANN are used to learn the system. Furthermore, the neurofuzzy system can prevent the knowledge acquired through learning based on the fuzzy knowledge from being thrown into a black box. In addition, the neurofuzzy system is also capable of extracting fuzzy knowledge from numerical data since they allow incorporation of both numerical and linguistic data into the system.

Generally, these neurofuzzy systems have the following features:

- A fuzzy system is used to create a relevant perception perspective, which possesses very clear physical meanings.

- All the fuzzy rules are expressed by a group of weights of an ANN and can be adjusted in a more effective way.
- The nonlinear characteristic of the ANN endows the fuzzy model greater abilities to describe a given complex system.

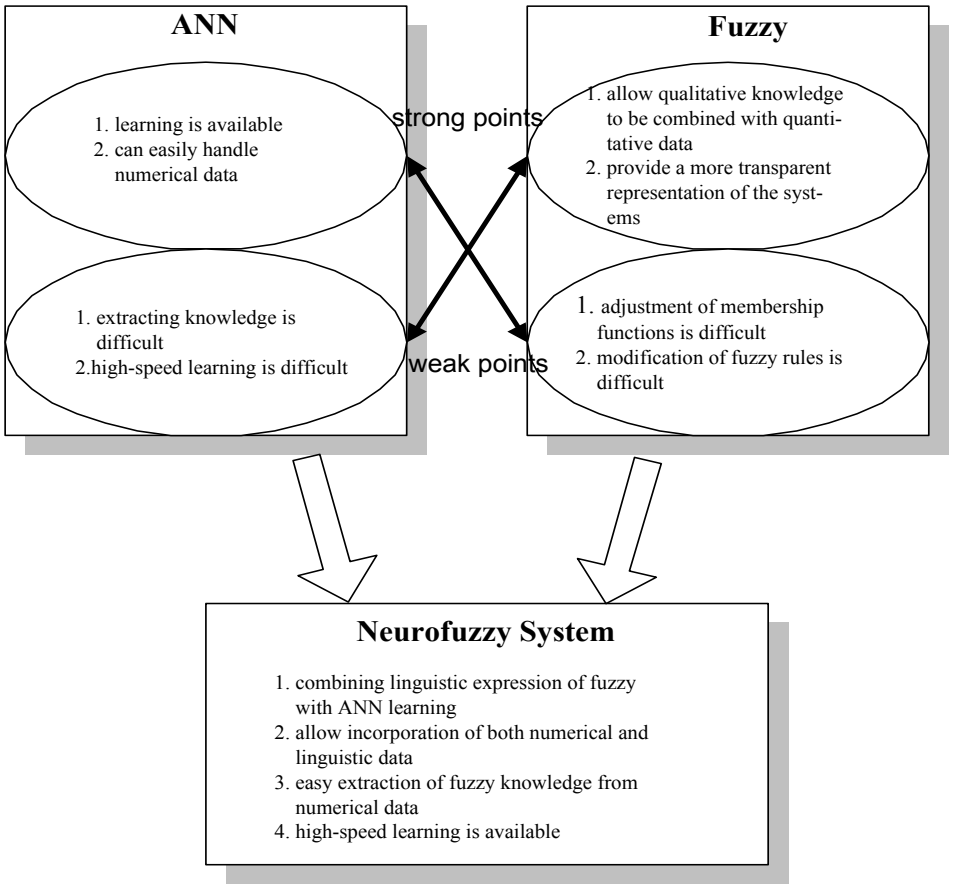

Figure 3.8: The comparative advantages of the neurofuzzy system.

The structure of dynamic neurofuzzy system (DNFS)

Dynamic NeuroFuzzy System (DNFS) developed by Hong etal. (2002) are usually applied to on-line tasks because of their good dynamic characteristics such as local generalisation, on-line clustering, on-line creating and updating of rule nodes and fast 'one-pass' training process. It inherits, improves, and extends the dynamic characteristics of general neurofuzzy system. DNFS has three learning modes: one on-line mode and two off-line modes. These modes can be applied to off-line, static systems and on-line, dynamic systems.

DNFS that is implemented for this project has the following characteristics:

- A dynamic Takagi-Sugeno fuzzy inference engine built dynamically.
  The Takagi-Sugeno fuzzy inference engine is used in both on-line and off-line modes of DNFS. The difference between them is that for forming a dynamic inference engine, only first-order Takagi-Sugeno fuzzy rules are employed in DENFIS on-line mode and both first-order Takagi-Sugeno fuzzy rules and expanded high-order Takagi-Sugeno fuzzy rules are used in DFNS off-line modes. To build such a fuzzy inference engine, several fuzzy rules are dynamically chosen from the existing fuzzy rule set depending on the position of current input vector in the input space.
- Dynamic creation and updating of fuzzy rules.
  All fuzzy rules in the DNFS on-line mode are created and updated during a 'one-pass' training process by applying the artificial neural network and the weighted recursive least square estimator with forgetting factors (WRLSE).

- Local generalisation.
  DNFS model has local generalisation to speed up the training procedure and to decrease the number of fuzzy rules in the system.
- Fast training speed.
  In the DNFS on-line mode, the training is a 'one-pass' procedure and in the off-line modes, WLSE and small-scale multi-layer perceptron (MLP) neural networks are applied, which lead DNFS to have the training speed for complex tasks faster than some common neural networks or hybrid systems such as multi-layer perceptron with back-propagation algorithm (MLP-BP) and Adaptive Neural-Fuzzy Inference System (ANFIS), both of which adopt global generalisation.
- Satisfactory accuracy.
  Using DNFS off-line modes, we can achieve a high accuracy especially in non-linear system identification and prediction.

The software of dynamic neurofuzzy system for the cooling water discharge modelling system was developed in MATLAB™ 6.1 environment.

3.3 Model Development and Results

Data set

The data set used in this study was collected from Tasman District Council (TDC) (pers. comm. Joseph Thomas and Martin Doyle). The following is a list of variables that is used in the modelling work:

- Rainfall at Kellings Road (site No.: 132010)
- Groundwater level at Palmers (site No.: 1219435)
- Total abstraction data in Moutere Western Groundwater Zone (OMWG in index of Tasman District Council).

All variables are averaged weekly for the modelling purpose.

Development of the dynamic neurofuzzy model

A dynamic model assumes that the new system can be predicted by the past inputs and outputs of the system. The ARX (AutoRegressive with eXogenous) model representation is a well known linear dynamic model, while the NARX (Nonlinear ARX) model is an extension that represents the model as a nonlinear mapping of past inputs and outputs to future outputs. Consider a predictive modelling for groundwater dynamics at Palmers as a multi-input, single-output (MISO) model with n_i inputs and n_o output. This system will be approximated by a collection of coupled discrete-time fuzzy models. The NARX model for a MISO dynamic system can be represented by:

$$y(k+1) = f\begin{pmatrix} u_1(k-n_{k_1}),....,u_1(k-n_{k_1}-n_{u_1}+1),...., \\ u_m(k-n_{k_m}),....,u_m(k--n_{k_m}-n_{u_m}+1) \end{pmatrix} \qquad \textbf{(5)}$$

$$k = 1,\ 2,\ \ldots\ldots,\ n$$

Here $y(k) \in Y \in R$ is the output vector, $u(k) \in U \in R^m$ is the inputs vector with *m* inputs. *n* and *k* denote the number of data samples and the discrete time samples, respectively. n_{u_m} is related to the system order. n_{k_m} represents the pure time delay between change in the inputs and the observed change in the output. $f(\cdot)$ is a nonlinear arbitrary function which can map the past inputs to future outputs.

The most important choice that has to be made is the model structure parameters (n_{u_m} and n_{k_m}). n_{k_m} represents the time delay between change in the inputs (rainfall and abstraction) and the observed change in the groundwater level at Palmers. A model free test proposed by He and Asada (1993) is used in this work. This method is based on the evaluation of the so-called *Lipschitz Quotients*.

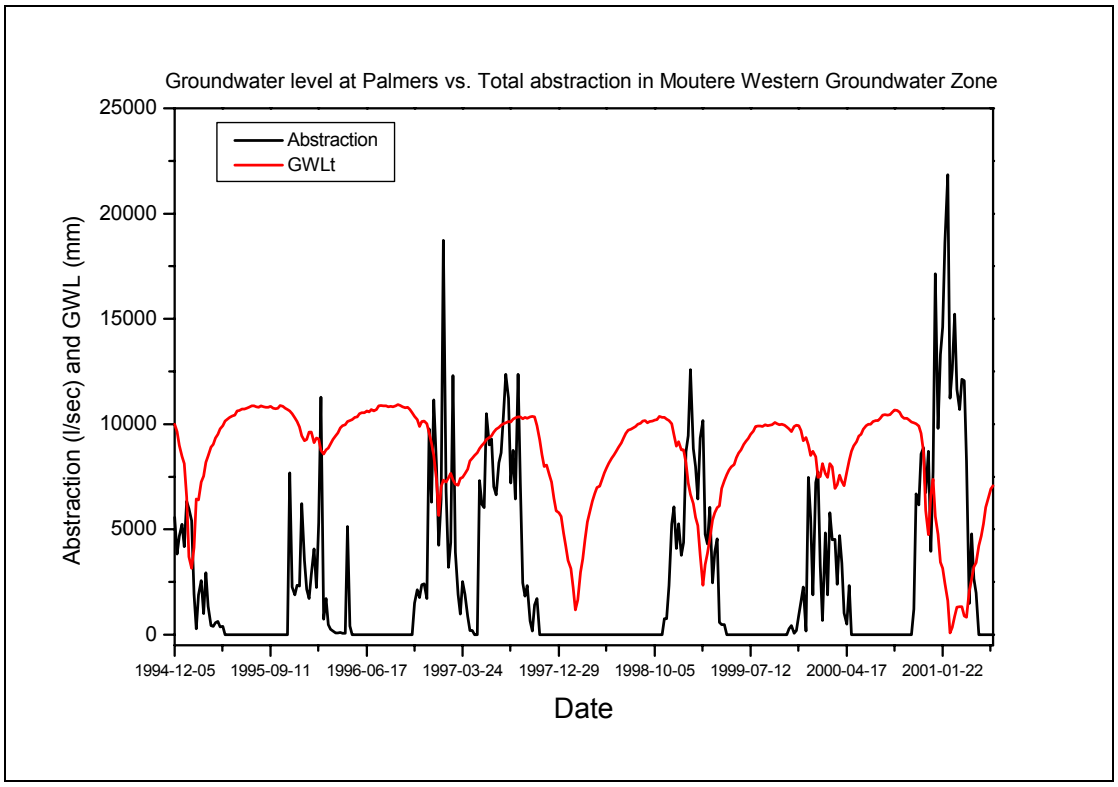

Figure 3.9: Abstraction vs. groundwater level at Palmers.

Figure 3.9 shows the graphical display of abstraction vs. groundwater level at Palmers. The *Lipschitz Quotients* method is done to find past input variable (abstraction) for the dynamic neurofuzzy model construction. The results of the *Lipschitz Quotients* method are shown in Figure 3.10. It is reasonable that the dynamic neurofuzzy model can be modelled by a first order model because the slope of the curve is decreased for model orders ≥ 3. The lag time between change in groundwater level at Palmers and increase in abstraction is approximately 3 day. The slope of the curve in Figure 3.10 is nearly flat after 6 of past abstraction input. The time span over which a momentary abstraction change persists in affecting the groundwater levels at Palmers is 1-6 weeks. The same procedure of *Lipschitz Quotients* method that adopted for abstraction data was applied to find past rainfall lag variables. It is found that previous 1-2 weeks rainfalls correlate strongly with the current groundwater levels at Palmers (see Figure 3.11). Mathematically, the multi-input, single-output (MISO) dynamic neurofuzzy model for the groundwater level dynamics at Palmers is described by:

$$\hat{GWL}(k) = f\begin{pmatrix} Abs(k-3), Abs(k-4), Abs(k-5) \\ Abs(k-6), Ra(k-1), Ra(k-2) \end{pmatrix} \quad (6)$$

where $\hat{GWL}(k)$ is the predicted groundwater level at time *k*. *f(.)* is a neurofuzzy model of the Takaki-Sugeno type. *Ra(t-1)* represents the rainfall at past one week .*Abs(t-3)* also means the rainfall at past three week. The dynamic neurofuzzy model has 1 output variable and 5 input variables.

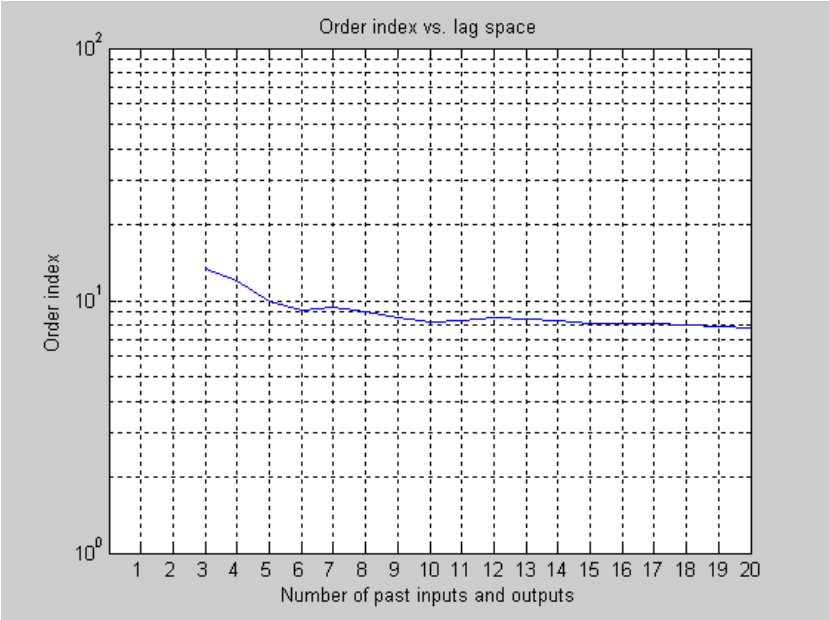

Figure 3.10: Results of lag time selection between abstraction and groundwater levels at Palmers by *Lipschitz quotients* method.

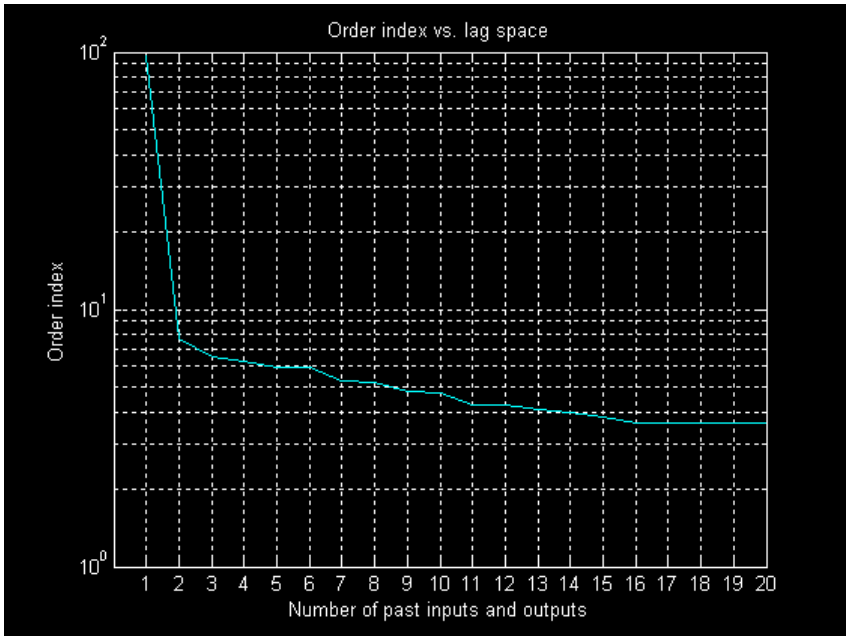

Figure 3.11: Results of lag time selection between rainfall at Kellings Rd. and groundwater levels at Palmers by *Lipschitz quotients* method.

Calibration result of the dynamic neurofuzzy model

Calibration results with observed groundwater levels at Palmers obtained from the dynamic neurofuzzy model are shown in Figure 3.12. Through Figure 3.12, the dynamic neurofuzzy model has a good generalisation capability for both wet season and very dry season. It can be seen that predicted results using the dynamic neurofuzzy model are in good agreement with values of observed groundwater levels and represent the dynamic characteristics of the given groundwater system very well.

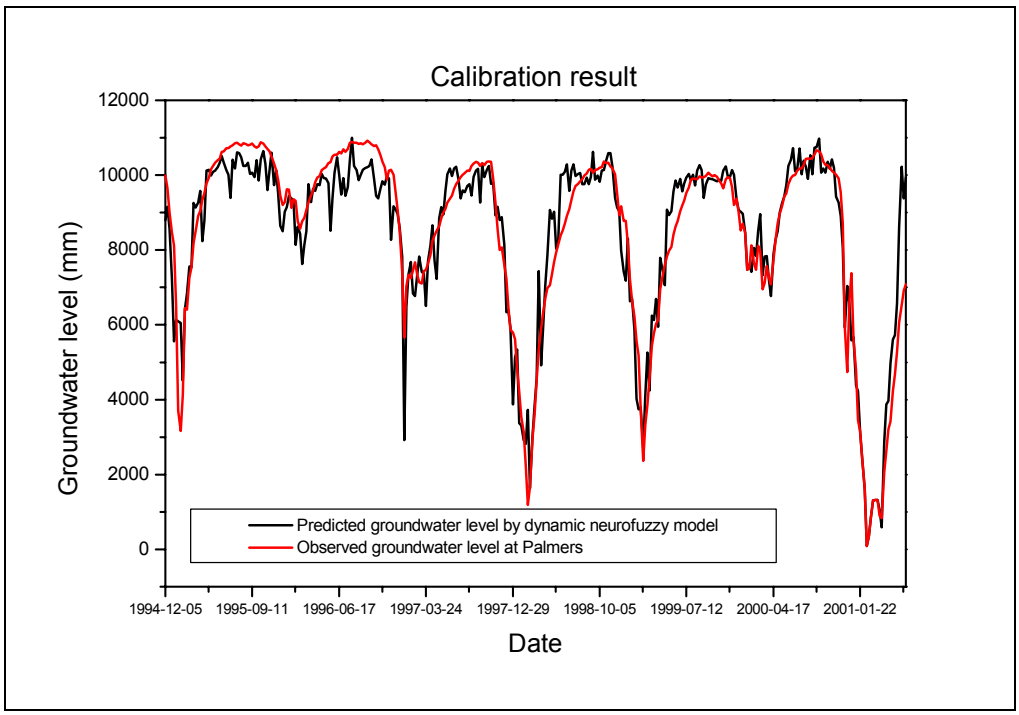

Figure 3.12: Prediction result of a dynamic neurofuzzy model with obsrevd groundwater levels at Palmers.

Scenarios simulation of the dynamic neurofuzzy model

The calibrated dynamic neurofuzzy fuzzy model developed in the previous section is used to assess the effects of different abstraction scenarios on groundwater level dynamics at Palmers. The abstraction scenarios that are used in the simulation are followings:

- scenario1 - no abstraction take in the period of 5/12/94 to 18/6/01,
- scenario 2 – 50% less take on the basis of historical abstraction take,
- scenario 3 - 50% more take on the basis of historical abstraction take,
- scenario 4 - 100% more take on the basis of historical abstraction take,
- scenario5 - maximum allowable abstraction take,

Summary of scenarios simulation

Figures 3.13 – 3.17 show the results of the effect of different abstraction on groundwater levels on Palmers discussed in the previous section. Table 3.1 shows the summary of simulation results of groundwater levels at Palmers based on different abstraction scenarios. Simulation results are extracted to analyse the effect of different abstraction on groundwater levels in the period of abstraction (Nov. – Apr.) during 1995-2001 years. From Table 3.1, increases in abstraction rate occur with decreases in the groundwater level at Palmers, or increases in the rainfall occur with increases in the groundwater level at Palmers. This is because the response of the groundwater level is the result of complicated interactions of recharge mechanism and abstraction.

In this report 1998 and 2001 years are referred to as ‘dry years’. 1996 year is referred to as a ‘wet year’. For the case of scenario1 (no abstraction at all) the groundwater level is entirely dependent on the rainfall event. Thus the simulation shows that the groundwater level at Palmers for the scenario1 keeps the steady-state level above 9000mm (9m) regardless of wet year (1996) or dry year (2001 and 1998).

When the groundwater levels are above 9m, the effect of more abstraction on groundwater levels would be significantly reduced. For example, at Nov. 1996 and Nov. 1998 decrease in groundwater levels due to 100% more take (scenario 4) would be just approximately 0.35m. In those periods several rainfall events were observed. Therefore the rainfall recharge process would prevent the significant decline of groundwater levels due to more abstraction. From Table 3.1, however, it can

be seen that the significant decrease in groundwater levels between January and March due to increase in abstraction (scenarios 3 and 4) would occur when/if the groundwater level falls below 7m. For example, at January 2001 where the observed groundwater level is 3.975m, the groundwater level for scenarios 3 and 4 would decrease from 3.975m to 1.998m and to 0.33m, respectively. This significant drop of the groundwater levels due to more abstraction in the dry season shows the important role of rainfall recharge process as a groundwater source in Moutere Western Groundwater Zone.

It is predicted that for 1995 - 2001 years the decrease in groundwater levels based on the scenario4 (100% more take) during January and March would be approximately 2.7m and up to 4.3 m (January 1999). For the case of scenario3 (50% more abstraction on the basis of historical take), the decrease in groundwater levels would be the average of 1.7m and up to 2.8m.

The interesting thing to observe is the response of groundwater levels in the dry year. The prediction shows that if the 50% less abstraction take (scenario2) occur the groundwater levels at Palmers is to increase from 3.975m to 7.15m (3m increase) in January 2001 and also from 0.732m to 4.6m in February 2001. On the other hand, the predicted groundwater levels between January 2001 and April 2001 would be dry compared to the historical observed groundwater levels with scenario4.
For the case of scenario5 (a maximum allowable abstraction take) the prediction shows that the groundwater levels in the period of January to April would be approximately 2.6m regardless of wet or dry year.

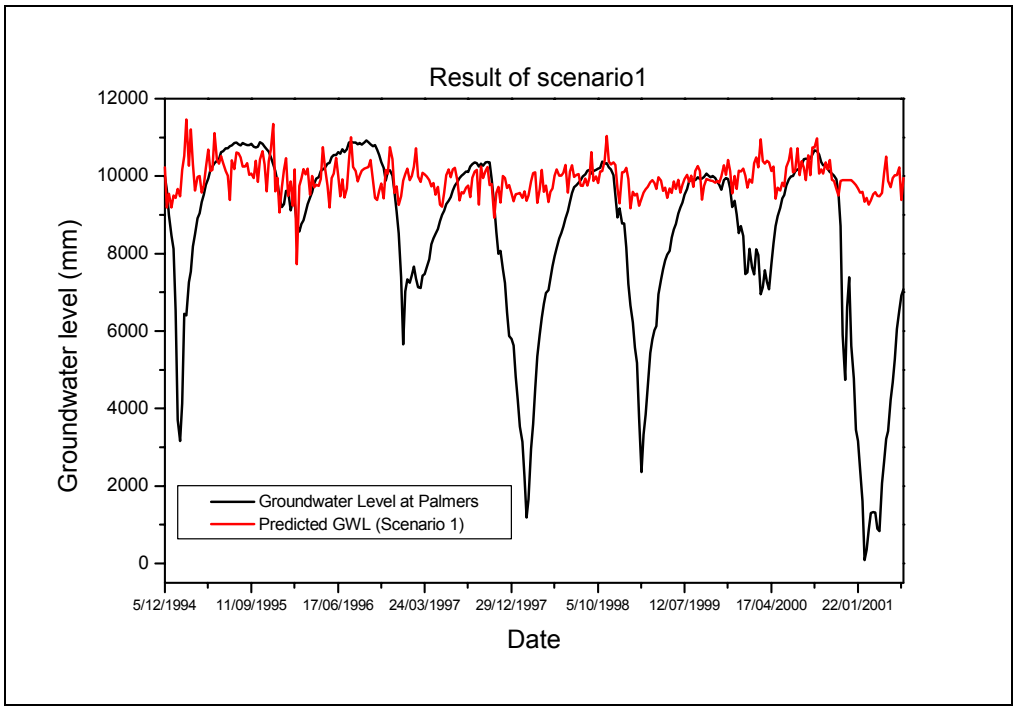

Figure 3.13: Simulation result of the dynamic neurofuzzy model with a scenario 1 (no abstraction take in the period of 5/12/94 to 18/6/01).

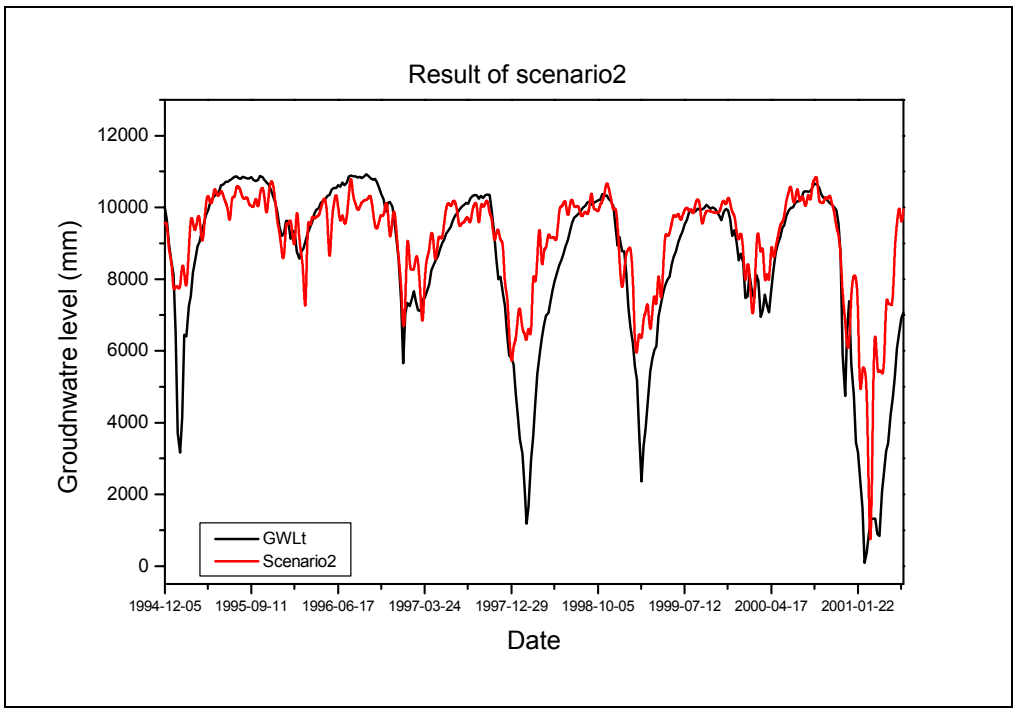

Figure 3.14: Simulation result of the dynamic neurofuzzy model with a scenario 2 (50% less take on the basis of historical abstraction take).

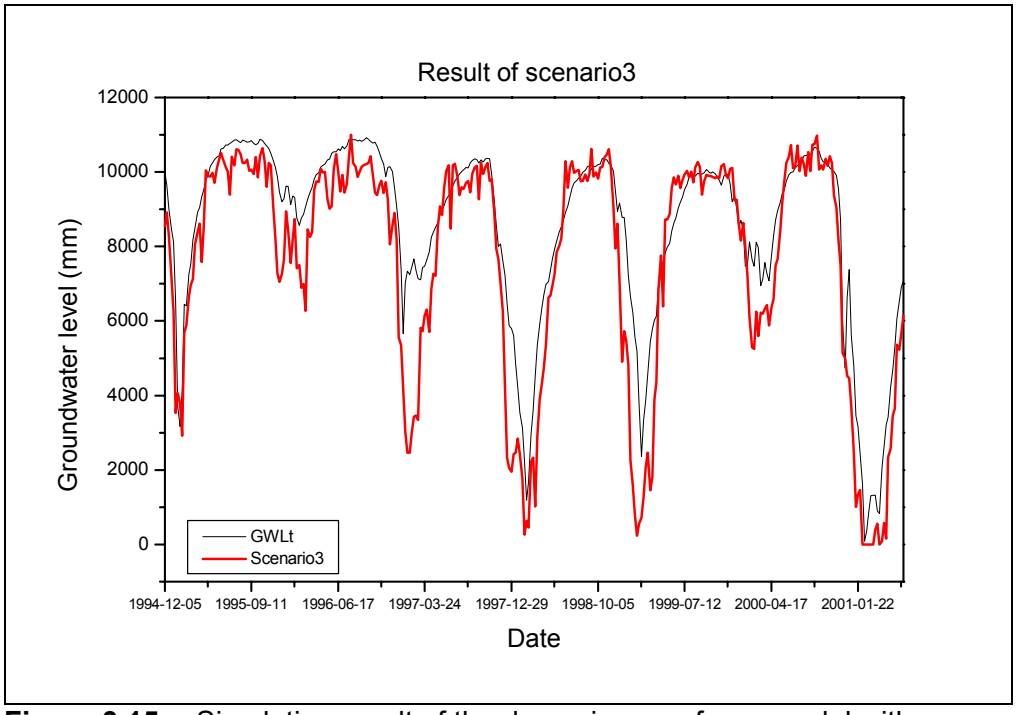

Figure 3.15: Simulation result of the dynamic neurofuzzy model with a scenario 3 (50% more take on the basis of historical abstraction take).

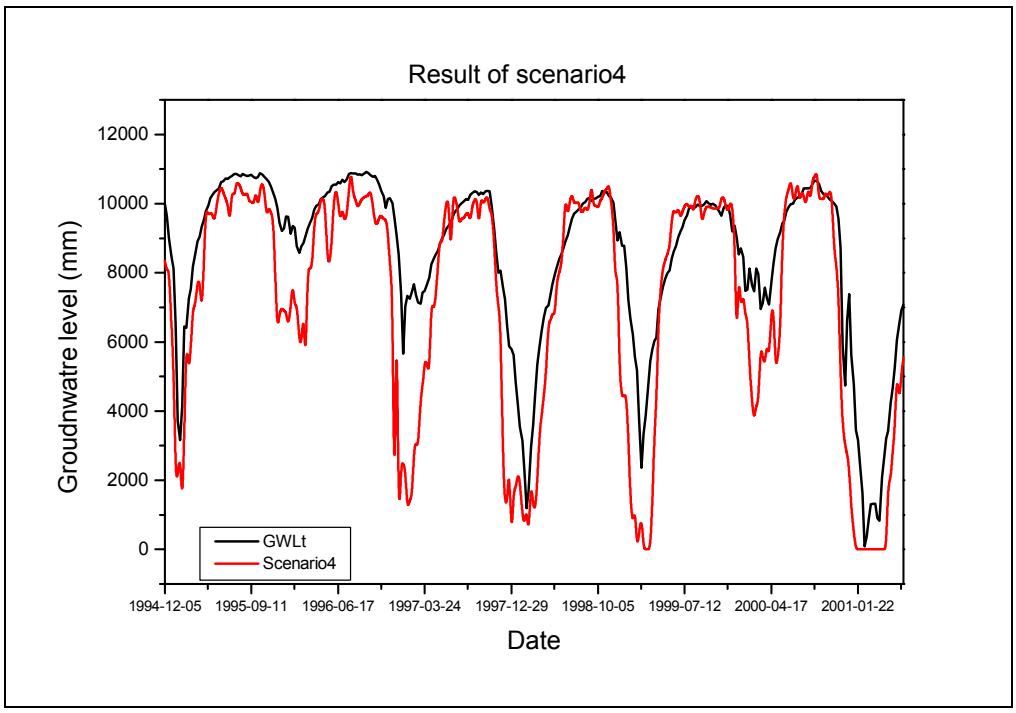

Figure 3.16: Simulation result of the dynamic neurofuzzy model with a scenario 4 (100% more take on the basis of historical abstraction take).

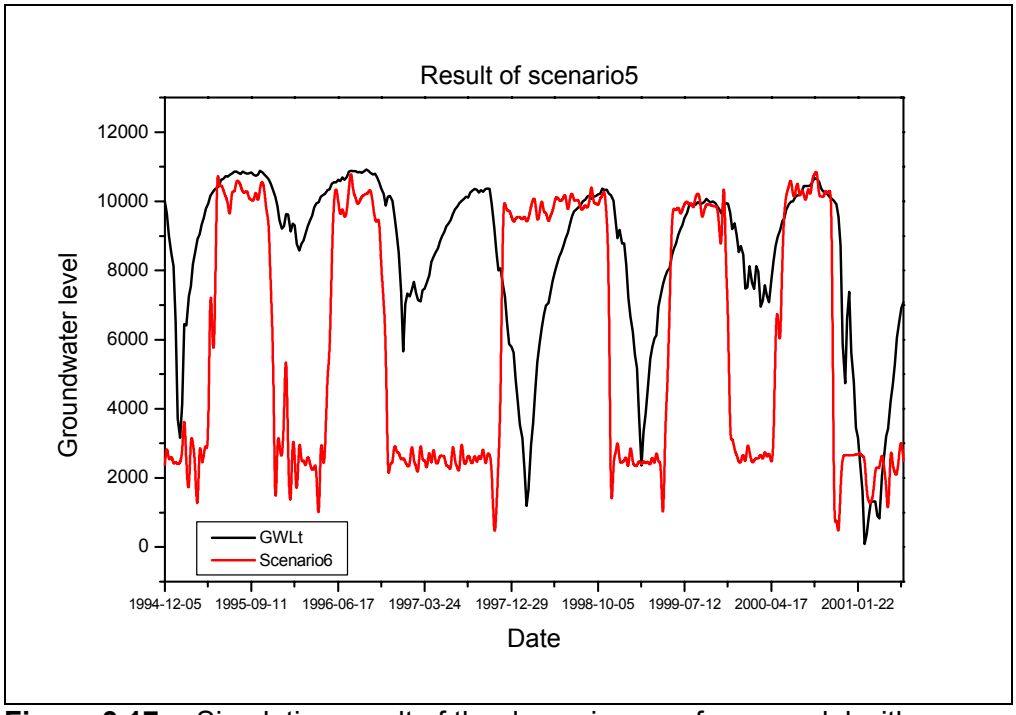

Figure 3.17: Simulation result of the dynamic neurofuzzy model with a scenario 5 (maximum allowable abstraction take).

year	GWL at Palmers	Jan	Feb	Mar	Apr	Nov	Dec
1995	Observed	5131	6914	8663	9644	10393	9452
	Scenario 1	9653	10870	9982	10061	10509	9729
	Scenario 2	7881	8602	9603	9680	10513	9699
	Scenario 3	4109	6298	8048	9017	9435	7311
	Scenario 4	2699	5127	7402	8643	9272	6757
	Scenario 5	2459	2797	2353	2615	5704	3105
1996	Observed	9083	8201	9292	9806	9865	8821
	Scenario 1	9846	9402	9943	9985	9868	9951
	Scenario 2	9368	9062	9609	9963	9996	9494
	Scenario 3	8380	7201	7848	9616	9550	7856
	Scenario 4	7004	6514	7386	9847	9487	4855
	Scenario 5	3128	2379	2388	2153	5701	2685
1997	Observed	6142	7148	7367	7926	8940	6133
	Scenario 1	9908	10217	9996	9745	9384	9794
	Scenario 2	7769	8359	7847	8893	10989	9170
	Scenario 3	3757	4193	5464	6761	7889	4360
	Scenario 4	2120	3636	4572	6565	7535	3595
	Scenario 5	2474	2563	2454	2658	1787	9794
1998	Observed	4289	2772	4751	7489	9982	7906
	Scenario 1	9499	9480	9801	9712	10474	9800
	Scenario 2	7293	6710	6520	8123	10296	8943
	Scenario 3	2536	782	2470	5261	9638	6575
	Scenario 4	1936	109	1965	4999	9654	5494
	Scenario 5	2499	2480	2801	4712	7604	3642
1999	Observed	6875	3566	5198	6968	10021	9642
	Scenario 1	9725	9425	9738	9840	10115	9840
	Scenario 2	8711	6167	6988	7585	10101	9772
	Scenario 3	3532	2472	2807	5714	9992	9673
	Scenario 4	2478	1672	2245	5499	9971	8718
	Scenario 5	2583	2397	2494	2539	8766	2893
2000	Observed	8311	7954	7985	7538	8917	6285
	Scenario 1	10035	10143	10474	10288	9732	9897
	Scenario 2	8702	8402	8708	8423	9846	6629
	Scenario 3	8121	5723	6085	6311	8515	4780
	Scenario 4	7176	4380	5240	6352	7331	2911
	Scenario 5	2610	2561	2647	2600	756	2659
2001	Observed	3975	732	1251	3056		
	Scenario 1	9753	9411	9496	9900		
	Scenario 2	7156	4602	4825	6239		
	Scenario 3	1998	0	240	631		
	Scenario 4	330	0	0	392		
	Scenario 5	2682	2026	1840	1954		

Table 3.1. Summary of monthly averaged groundwater levels at Palmers with different abstraction scenarios.

CHAPTER 4: SURFACE RECHARGE IN THE WAIWHERO CATCHMENT

It is believed that parts of the Waiwhero catchment are in the recharge zone for the Moutere groundwater system (Thomas, 1989). In order to investigate this further two studies have been undertaken:

- An investigation of the soil water balance under pasture and pine forest in the Waiwhero catchment; and
- A shorter study investigating the possibility of recharge from the stream channel.

4.1 Description of Waiwhero Catchment

The Waiwhero is a small east flank tributary of the Motueka River with a catchment area of 92 km^2. It has predominantly hilly terrain, underlain by Moutere gravels. At the western margin of the catchment, before joining the main stem Motueka, there is an area draining Separation Point granite. Moutere gravels are a claybound, deeply weathered gravel, of late Pliocene to early Pleistocene age (< 2 Ma) up to 300 m thick. Moutere gravels are dominated by greywacke sandstone clasts, mainly <200 mm diameter, in a silty clay matrix. The Moutere gravels have a transmissivity of 3 to 120 m^3/day/m. The two major land uses in the Waiwhero catchment are pastoral farming and exotic plantation forestry.

4.2 Soil Water Balance under Pasture and Pine

In order to characterise the water use differences between pasture and forestry on the Moutere aquifer recharge zone two sites were instrumented and sampled for a water balance analysis. The first site was pasture in a first order catchment in the upper Waiwhero. The second site was under mature Pinus radiata plantation, also in the upper Waiwhero. The field study was carried out between May 1997 and September 1999. The instrumentation was:

- 15 Neutron probe access tubes for soil moisture measurements at each site. Positions for the access tubes were chosen to represent a range of slope positions.
- Tensiometers were installed for a short period to gain an understanding of soil moisture change between neutron probe readings and hydraulic gradients.
- Soil samples were taken and analysed for soil physical properties (dry bulk density; rooting depth; saturated hydraulic conductivity)
- Sapflow meters were installed on the pine trees to measure transpiration rates.

The data were used to parameterise a water balance model to assess the possibility of groundwater recharge occurring from these sites.

Soil physical properties

In figure 4.1 it can be seen that soil dry bulk density increases rapidly with depth and is greater than 1.5 t/m^3 in all B horizons below 0.3 m depth. The forested sites have a slightly lower dry bulk density than pasture, although this is only evident in the top 30cm. This is consistent with other studies and reflects the higher organic content in forest soils.

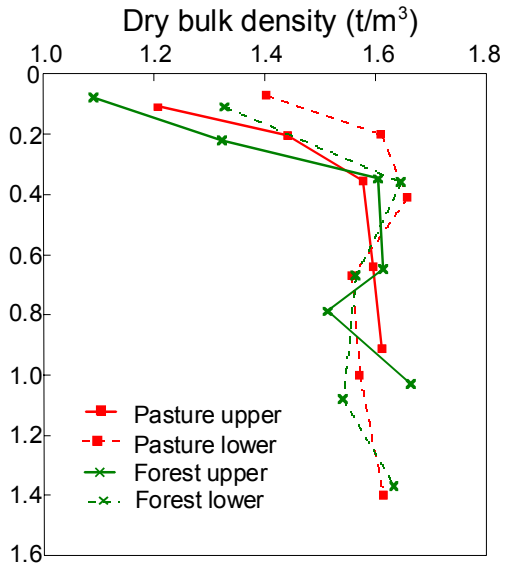

Figure 4.1: Dry bulk density changes with depth (in metres)

Under both pasture and pines, roots are abundant (figure 4.2) in A horizons and less in the B horizons. Rooting depths were similar between pasture and pines with roots being present to approximately 1 m with root concentrations <1 cm/cm^3 below 0.3 m depth.

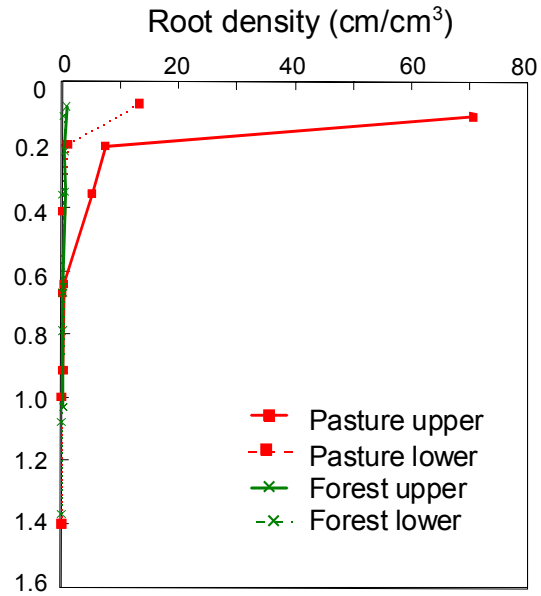

Figure 4.2: Root density with depth (in metres)

Saturated hydraulic conductivity measurements (using ring infiltrometers) indicate very low potential movement rates, typically less than 1mm an hour at depths below 1 metre (figure 4.3). These values indicate that it would take a long time for water to infiltrate through the surface to recharge groundwater. It is possible that bypass flow increases the rate of infiltration at places, but potentially it would take 10-80 days for water to travel 2 metres.

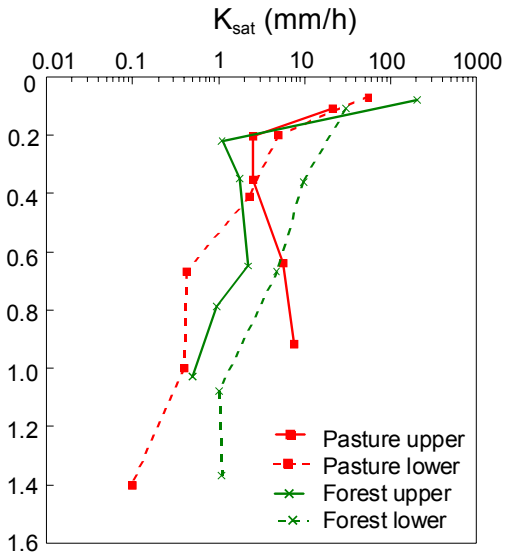

Figure 4.3: Saturated hydraulic conductivity with depth (in metres)

By looking at the difference in water content between the wettest and driest period the total available water (i.e. maximum storage of water in the soil) can be determined. For both sites the total available water is estimated at 150mm.

Field observations

Observations of the water table indicate that a perched water table is often present in B horizons in winter on lower slopes, and for short periods during rainfall on upper slopes.

Most rainfall infiltrates at the soil surface, but surface runoff occurs on dry surfaces in summer. Most of this surface runoff redistributes on the slope and reinfiltrates.

During the summer, evaporation exceeds rainfall and dry soils limit transpiration of pines and pasture; in winter, rainfall exceeds evaporation and surplus water drains to streams and potentially to groundwater.

Modelling results

The model used in this work simulates the daily water balance using the water balance equation:

$$P - E - Q \pm \Delta S = 0$$

where P is precipitation; E is evapo-transpiration; Q is runoff; and ΔS is change in storage.

Precipitation is taken from daily rainfall records. Evapo-transpiration is calculated from potential evaporation values and scaled to the appropriate vegetation type. Change in storage is based on a filling and draining of two stores: the surface soil and a baseflow store. The size of surface store is defined by the available water capacity, which is derived from the difference between the wettest and driest soil moisture profile. Water is able to be extracted from this surface store for evapo-transpiration. The baseflow store only fills when the surface store is completely filled. It's size and how it drains as baseflow are described by hydrological properties derived from the streamflow record (baseflow index and recession coefficient). Runoff is assumed to be the water surplus after accounting for the other three variables. A full description of the model can be found in Fahey (2003).

Figure 4.4 shows the simulated surface storage as compared to the measured surface storage (neutron probes) for the pasture site. The labelling of this diagram has assumed that the surface storage is equal to the soil moisture storage. The point measurements of surface storage agree well with the simulated storage, although the model appears to dry out too much in the summer. Of particular importance for a study of groundwater recharge is how well the autumn and winter are

simulated, as these are critical periods for potential deep infiltration of water. In this case these periods are well simulated.

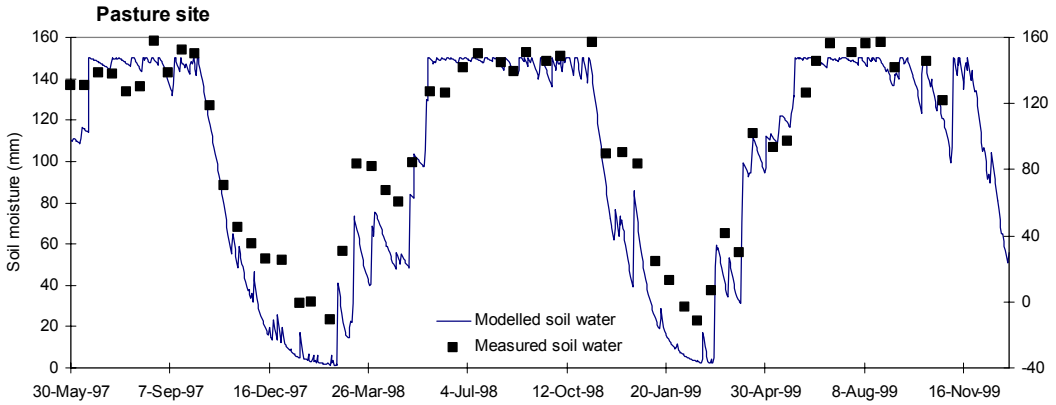

Figure 4.4: Measured and simulated surface storage (soil moisture – see text) for the pasture site.

Figure 4.5 is similar to figure 4.4 except it is the simulation and measurement at the forest site. The difference between simulations here is in the evapo-transpiration part of the water balance where there is a consideration of rainfall interception and different transpiration rates. The model is simulating the soil moisture time series well when compared to point measurements, although there are less winter measurements to compare with.

Overall the model appears to perform well as a simulator of surface storage.

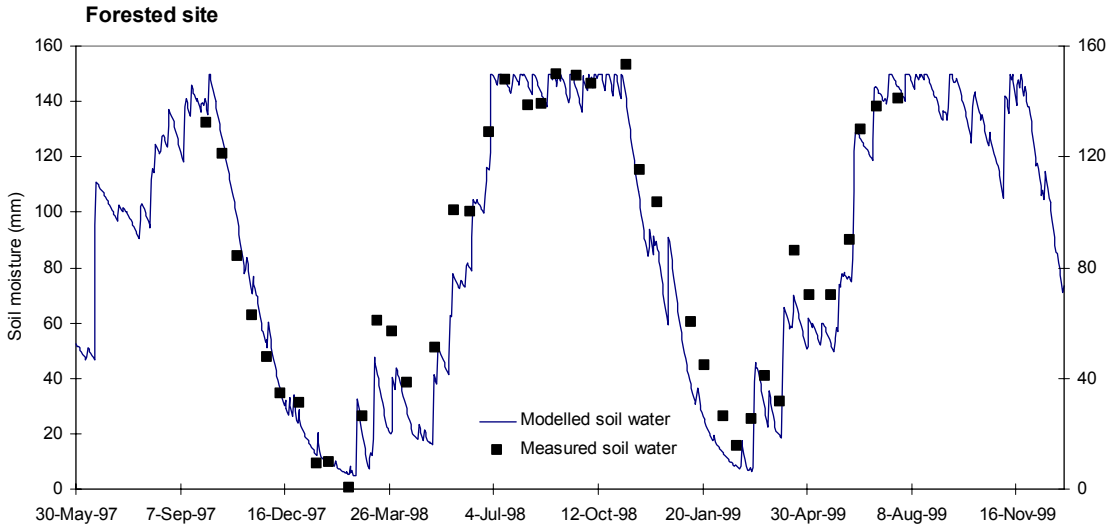

Figure 4.5: Measured and simulated surface storage (soil moisture – see text) for the forest site.

In figure 4.6 the two simulations are combined for comparative purposes n.b. although the simulations appear to start on June 1st, 1997 they actually start well before this to allow the model to overcome initial boundary conditions. In figure 4.6 it is evident that the pasture and pine sites have a very similar time series through the spring and summer. This is a reflection of a similar transpiration rate and rooting depth (as evidenced in figure 4.2). It is also evident that both the pasture and forest sites reach a period of full storage during the winter, although the pasture reaches this point considerably faster than the forest. During the summer months all the available rainfall is immediately taken for transpiration. During the autumn period the lesser amount of rainfall available after canopy interception and evaporation from the wet forest canopy) means it takes longer to fill the surface store. This is a critical finding from the study as it is only when the surface store is filled that infiltration of rainwater can start to recharge the baseflow store. The

delay in filling the surface store means that the groundwater recharge under a forested site will occur over a much shorter period of the winter than for pasture.

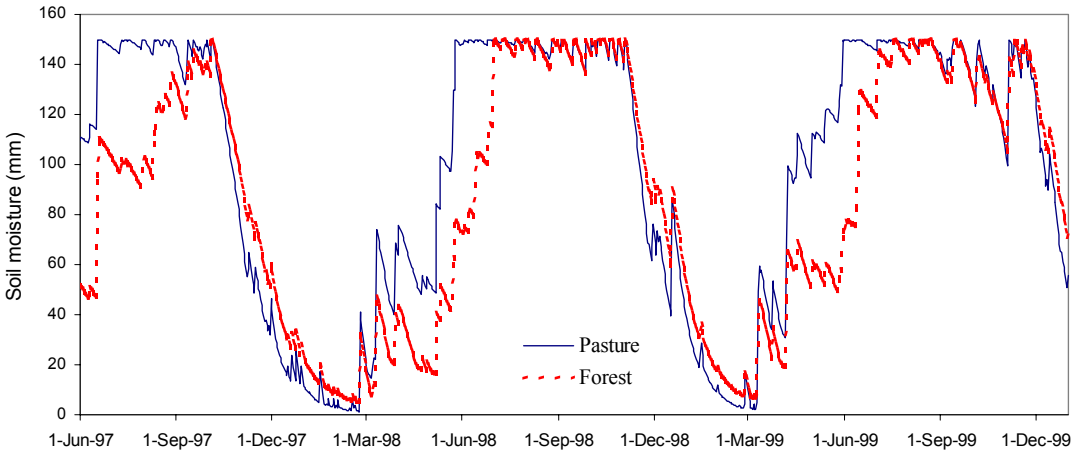

Figure 4.6: Simulated surface storage for pasture and pines during the period of study.

The modelled streamflow, compared to measured streamflow, can be used as a crude method to explore the amount of possible groundwater recharge occurring. The model is a closed system; it assumes that there are no losses of water other than through streamflow (runoff) or evaporation. There is a shallow groundwater store but it is assumed to provide baseflow for the stream and allows no losses to a deeper regional groundwater. Conceptually this model does not represent a system where there are possible losses of water to the Moutere aquifer. Therefore discrepancies between what the model predicts and measured streamflow may be indicative of groundwater recharge losses. In other words if the water balance equation was changed so that:

$$P_m - E_s - Q_m \pm \Delta S_s = G_s$$

where the subscript *m* refers to "measured"; *s* to "simulated" and G is groundwater recharge. In this case measured streamflow is being substituted for simulated streamflow and the difference assumed to be groundwater losses. It is only sensible to do this for the period when potential groundwater recharge may occur: the winter when surface storage is full. The measured streamflow is the Waiwhero weir at Poplars, which has a catchment area of 84 hectares over pasture.

In figure 4.7 simulations from the 1999 wet period (June through to October) are shown. It is immediately apparent that there are discrepancies between observed and simulated. The model over predicts the size of peak events and does not simulate the recession limb from these peaks very well. During August there are a series of small storms that cause only a very small rise in the observed hydrograph but quite large peaks in the simulated. The over prediction and flashiness of simulated storm hydrographs suggest that the model is keeping the surface store very wet and responding instantly to rainfall. The fact that this isn't happening in the observed hydrographs may be due to deep drainage from the stores allowing more of the storm rainfall to be absorbed and then slowly let out i.e. a larger baseflow store that allows drainage from it's base. The amount of water flowing as baseflow (i.e. between storm events after the recession limb flattens out) is well simulated. Overall this suggests that the model is conceptually wrong in having a closed store system.

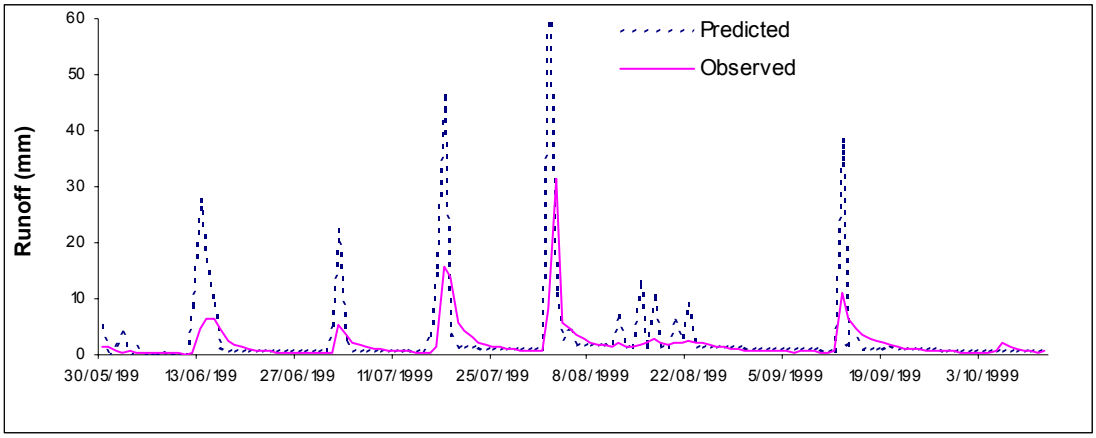

Figure 4.7: Simulated and observed streamflow for the winter period of 1999. Streamflow is from the Waiwhero Poplars weir.

If the seasonal totals in predicted and observed rainfall are totalled, the discrepancy between the observed and simulated recession limb is less important and the impacts of minor variations are lessened. In order to do this there is no set seasonal length, what is important is the length of period where the surface store is saturated and therefore groundwater recharge can occur. Results from this analysis are shown in table 4.1.

Wet period	Rainfall (mm)	Predicted runoff (mm)	Measured streamflow (mm)	Discrepancy (mm)	Discrepancy (mm/day)
21/6/97 – 9/10/97	247	159	119	+40	0.36
14/5/98 – 6/11/98	925	730	647	+83	0.47
30/5/99 – 16/11/99	715	498	327	+171	1.01

Table 4.1: Discrepancies between predicted and observed runoff for three wet periods.

In all of the periods there was a surplus of water, i.e. there was less water going down the stream than anticipated. This loss could be attributed to groundwater recharge but there are large errors involved in the assessment and it is not possible to give an accurate groundwater recharge amount. There are errors involved in all terms of the water balance equation; ie

- Estimating evaporation
- Estimating soil water storage
- Measuring streamflow
- Measuring precipitation.

These errors accumulate so that a detailed error analysis could show the surplus water as plus or minus 100%. However the evaporation is term is relatively small during the winter and a preliminary analysis of precipitation variation has shown a relatively small likely error (R. Jackson, pers. comm.).

The differences from year to year reflect the different type of winters during the study periods. The first winter was relatively dry with approximately 10 small storm events (where streamflow was above baseflow). The second winter was wet with approximately 20 storm events, including 4 large flow events. The third winter (see figure 4.7) was somewhere in between but had only 8

storm events, the majority of which were large. This suggests that if the discrepancy is due to groundwater losses the amount lost is variable, dependent on the type of winter experienced.

The amount of water potentially lost, ie.table 4.1, is quite small (40-171mm) but when applied over a large recharge area can produce large volumes of recharge. Over the relatively small Waiwhero catchment above the Rosedale gauging site (397 ha) this becomes betweem 159,000 – 680,000 m^3 of water during the wet period.

For the periods of wet shown in table 4.1 the model predicts that would have been considerably less runoff under the forest (7mm in the first winter; 330mm in the second and 179mm in the third). These results suggest that under complete cover of Pinus radiata the Waiwhero would not have been flowing for large periods of time during the winter of 1997 and would have had reduced flow during the other wetter winters. However it is quite possible that groundwater recharge would occur under the forest as the surface store did reach saturation in every winter. The amount of recharge is likely to be reduced by the fact that the surface store does not remain wet for as long as under a pasture cover.

Conclusions from modelling

Under a pastoral land use, a double store; closed system water balance model of the Waiwhero, over-predicts the amount of water flowing down the stream during the winter. It is possible that some of this over-prediction could be due to the system being open at the bottom and there are losses to deep groundwater. Reformulating the model to account for this and attempting to match the streamflow record with the revised model could investigate this.

Forest cover shortens the length of the time during the winter and spring when the surface store is fully wet (and therefore able to recharge groundwater). This potentially does affect the amount of groundwater recharge during the winter.

4.3 Streamflow Losses

The possibility of streamflow losses to groundwater in the Waiwhero catchment was investigated through an examination of permanent gauging records and spot gauging along the main stream.

Assessing streamflow record between permanent gauges

Tasman District Council (TDC) maintains a permanent flow gauging structure within the Moutere Gravel section of the Waiwhero. Due to the construction of holding ponds and dams within the catchment the gauge has had to be moved twice. Prior to moving the gauge there was an overlap of 21 months (June 1997 – March 1999) when both gauges were recording streamflow. This period of record has been examined to assess whether there are detectable streamlow losses between the gauges.

The upstream gauge was located at Poplars (referred to in diagrams here as Waiwher**P**); the catchment area above this point is 84.2ha. The downstream gauge was located at Rosedale (referred to in diagrams here as Waiwher**O**); the catchment area below this point has an area of 397 ha. The catchment of the Poplars gauge is part of the greater Rosedale gauge catchment. At the Poplars site it is a small zero order stream, at Rosedale it is a small first order stream.

Figure 4.8 shows the double mass curve of runoff for the period of overlap between stations (N.B. both stations are in mm so area has been equilibrated). It can be seen from this figure that there is a loss of water between the two stations and this increases through the period. The dashed red line in figure 1 shows an equivalent mass of water at both locations. For the hydrological year starting July 1997 the difference between the runoff at Poplars (185.8 mm total) and at Rosedale (163.6 mm total) is 22.3 mm. This amount of water equates to approximately 18,800 m^3 per year (or an average of 0.6 litres per second) of water that exited the Poplars weir but may not have reached the Rosedale weir site. N.B. The actual volume at Rosedale was higher than at Poplars, the assumption being made here is that the hydrologic response is the same throughout both catchments.

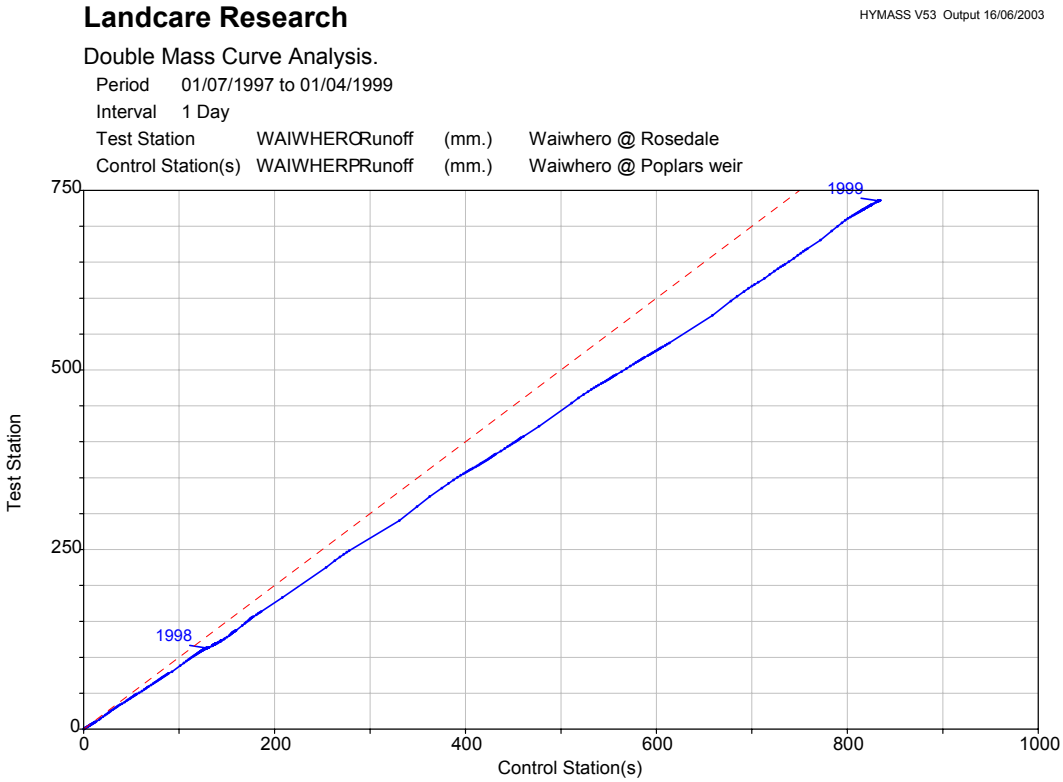

Figure 4.8: Double mass curve of runoff at Poplars (WaiwherP) and Rosedale (WaiwherO) for the period of overlapping records.

The consistent nature of difference between the two sites (figure 4.8) suggests a consistent error. Hydrograph separation shows that the same ratio of total flows exists between the two sites; irrespective of whether the flows are stormflow, baseflow or total flow (table 4.2). The remarkable similarity points to a consistent error such as the area calculations for one of the catchments being incorrect. If there was a channel flow loss it might be expected to show up as much higher ratio for baseflow than quickflow.

	Waiwhero - Rosedale	Waiwhero - Poplars	Ratio
Quickflow	309.5	351.9	1.14
Baseflow during highflow events	128.8	147.3	1.14
Baseflow between highflow events	296.5	333.7	1.13
Total flow	734.8	832.9	1.13

Table 4.2: Runoff totals (in mm) during the period March 1997 to June 1999. Hydrograph separation was carried out using the Hewlett method.

The differences between the two gauges are especially marked during peaks; the peaks at Rosedale are lower. This is to be expected since Poplar is a part of the Rosedale catchment and the reactions at the Rosedale gauge can be slower than at Poplars (due to greater distances of travel for the water).

Spot gauging measurements in the Waiwhero catchment

Spot gauging along the Waiwhero was carried out during October 2002 to see if there were any detectable losses. The results from these gaugings are shown in figure 4.9.

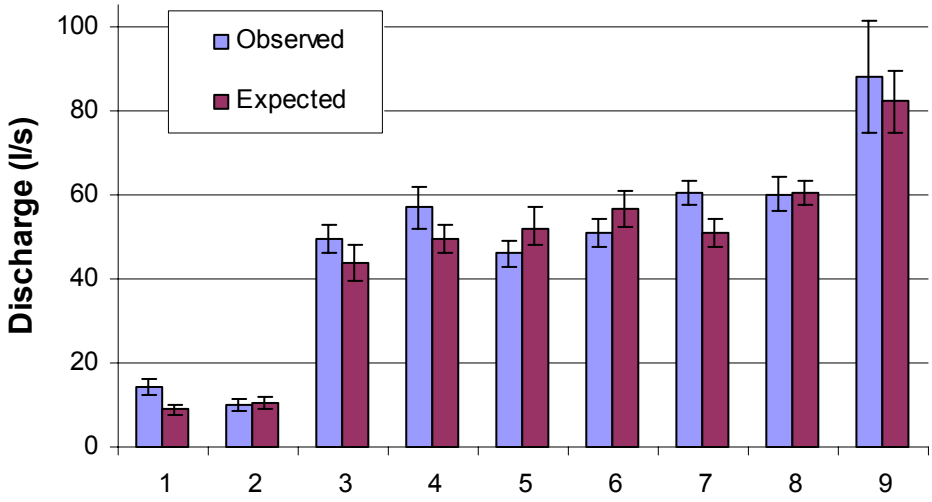

Figure 4.9: Flow gaugings down the Waiwhero. Expected results are calculated from additions of tributaries between measurements. Error bars are from the gauging calculations.

The results in figure 4.9 show that there were no detectable losses in river flow over the 3km stretch where readings were taken, i.e. the difference between observed and expected was never larger than the calculated error. The errors in measurement (calculated through accumulated errors from separate measurements) vary between 1 and 7 l/s. This suggests that it may be possible to detect losses at the high streamflow end of the scale but not during small runoff events or normal flows.

Conclusions

Analysis of streamflow from permanent structure gauges suggests that there may be a loss of flow from the Waiwhero streambed but the consistent nature of loss points to a calculation error rather than actual water loss. Spot gauging during the spring was not able to detect any losses. In the Waiwhero stream, channel losses cannot be considered a significant detectable groundwater recharge mechanism.

CHAPTER 5: SUMMARY & CONCLUSIONS

The Moutere aquifer system is an important source of groundwater for horticulture and other land uses in the Moutere valley and beyond. The ability of the aquifer to 'recover' following summer abstractions is dependent on adequate recharge mechanisms. In this report Moutere aquifer recharge has been investigated in three different ways:

- Dating the groundwater and inferring groundwater recharge mechanisms
- Modelling the groundwater interactions with precipitation and abstraction
- Studying the impact of different land uses in the hypothesised recharge zone

Dating the groundwater

Recharge to the Moutere Gravel aquifer system in the Moutere Valley was investigated by means of isotopic and chemical measurements. Shallow bores (50-100 m) have $\delta^{18}O$ in the range expected for present-day rainfall. Their carbon-14 concentrations generally indicate modern ages, i.e. water residence times of up to hundreds of years.

Deeper bores have more negative $\delta^{18}O$ values and lower ^{14}C concentrations resulting from input of much older water from depth in the western and eastern zones. The old deep water is believed to have been recharged in the Pleistocene during the last glaciation. Mixing of glacial and modern waters gives rise to the variations observed in the oxygen-18, carbon-14 and chemical concentrations in the bore waters. Sea level was much lower when the glacial water was recharged, and the sea would have been far from its present position. A large body of glacial water may be resident in the Moutere Gravel under the sea.

Recharge is provided by modern water penetrating the groundwater system at shallow levels. Measurements on this water give evidence on the patterns and rates of recharge. The distribution of $\delta^{18}O$ and chloride suggest that water has been recharged through both the tm1 and tm2 units of Moutere Gravel in the past few hundred years, but evidently at very low rates because of the ages. Young recharge is observed only on the hills west of the valley floor, but observations are lacking in the most probable recharge zone (the tm2 outcrop area in the Rosedale Hills).

Modelling abstraction and precipitation interactions

An empirical model of groundwater response to abstraction and precipitation has been developed using neural networks and fuzzy logic. The model is a good predictor of aquifer response to abstraction and precipitation during the winter months.

The model suggests that rainfall recharge is likely to be the main recharge mechanism. Scenario modelling suggests that even with a greater extraction rate than has occurred over the last 10 years, the aquifer is likely to recover during the winter. In interpreting this result sit is important to note that this assumes the same recharge mechanisms occur, i.e. their no reduction in the amount of recharge.

Impacts of land use

A double store-close system water balance model that has been calibrated for conditions in the Waiwhero catchment; part of the hypothesised Moutere aquifer recharge zone. Under a pastoral land use the model over predicts the amount of water flowing down the stream during the winter. It is possible that some of this over prediction could be due to the system being open at the bottom (i.e. not a closed system) and there are losses to deep groundwater. The amounts of water "lost" during a wet period are small when presented as water depths and easily accountable through measurement and estimation errors in the analysis. However when translated into volumes, through multiplying over a large recharge area, they are potentially significant in terms of groundwater recharge.

Forest cover shortens the length of the time during the winter and spring when the surface store is fully wet (and therefore able to recharge groundwater). This potentially does affect the amount of groundwater recharge during the winter.

Analysis of streamflow from permanent structure gauges suggests that there may be a loss of flow from the Waiwhero streambed but the consistent nature of loss points to a calculation error rather

than actual water loss. Spot gauging during the spring was not able to detect any losses. In the Waiwhero stream, channel losses cannot be considered a significant detectable groundwater recharge mechanism.

Overall conclusion

The groundwater extracted from the deep Moutere aquifer is very old (over 1000 years) but there are recharge mechanisms occurring that mean, even with high extraction rates, the aquifer is able to recover during the winter. The recharge is likely to be from surface infiltration throughout the Rosedale hills area. Although the surface infiltration will take many hundreds of years to reach the main Moutere aquifer it creates a sufficient pressure gradient to cause water levels to recover during the winter. Replacement of pasture with tall vegetation on the recharge area affects the amount of surface infiltration. This impact is through delaying the autumn/winter onset of a wet soil mantle (when surface infiltration to groundwater can occur) and lessening the volume of water available for recharge.

REFERENCES

Clark, I.D.; Fritz, P. (1997) Environmental isotopes in hydrogeology. Lewis Publishers, New York. 328 p.

He, X., and Asada, H. (1993) A New Method for Identifying Orders of Input-Output Models for Nonlinear Dynamic Systems. *Proc. of the American Control Conf*., S.F., California.

Hong, Y.-S., Rosen, M. R., and Reevs, R. R (2002) Dynamic fuzzy modelling of strom water infiltration in urban fractured aquifers. *Journal of Hydrologic Engineering*, American Society of Civil Engineers, Vol.7, No. 5, 380-391.

Hulston, J.R.; Taylor, C.B.; Lyon, G.L.; Stewart, M.K.; Cox, M.A. (1981) Environmental isotopes in New Zealand hydrology. Part 2. Standards, measurement techniques and reporting of measurements for oxygen-18, deuterium and tritium in water. *New Zealand Journal of Science 24,* 313-322.

Jang, J.-S. R. (1993) ANFIS: Adaptive-network-based fuzzy inference systems. *IEEE Trans. Systems, Man & Cybernetics*, 23(3), 665-685.

Lihou, Joanne C. 1992: Reinterpretation of seismic reflection data from the Moutere Depression, Nelson region, South Island, New Zealand. *New Zealand Journal of Geology and Geophysics 35*, 477-490.

Mamdani, E. H. (1974) Application of fuzzy algorithms for control of simple dynamic plant. *Proc. of IEEE*, 121, No 12, 1585.

Rattenbury, M.S., Cooper, R.A., Johnston, M.R. (compilers) (1998) Geology of the Nelson Area. Institute of Geological and Nuclear Sciences 1:250,000 geological map 9. (1 sheet + 67 p.) Lower Hutt, New Zealand.

Rosen, M.R. (2001) Hydrochemistry of New Zealand's aquifers. *In* Groundwaters of New Zealand, M.R. Rosen and P.A. White (*eds*). New Zealand Hydrological Society Inc., Wellington. Pp. 77-110.

Stewart, M.K.; Dicker, M.J.I.; Johnston, M.R. (1981) Environmental isotopes in New Zealand hydrology. Part 4. Oxygen isotope variations in subsurface waters of the Waimea Plains, Nelson. *New Zealand Journal of Science 24,* 339-348.

Stewart, M.K., Morgenstern, U. (2001) Age and source of groundwater from isotope tracers. *In* Groundwaters of New Zealand, M.R. Rosen and P.A. White (*eds*). New Zealand Hydrological Society Inc., Wellington. Pp. 161-183.

Stewart, M.K. (2002) Moutere Valley Groundwater: Nature and Recharge from Isotopes and Chemistry. IGNS Science Report 2002/22. 31p.

Stewart, M.K., Trompetter, V., van der Raaij, R (2002) Age and source of Canterbury Plains groundwater. Technical Report, Environment Canterbury.

Takagi, T., and Sugeno, M. (1985). Fuzzy identification of systems and its applications to modeling and control. *IEEE Trans. Syst., Man & Cybernet*., 15, 116-132.

Thomas, J.T. (1989) Hydrogeology of the Moutere Valley, Nelson, New Zealand. Unpublished MSc Eng. Geol. Thesis. Department of Geology, University of Canterbury, New Zealand.

Thomas J.T. (1989) Groundwater Investigations in the Moutere Catchment. Proc. NZ Assoc. of Soil and Water Conservation, Annual Conference, Nelson. Pp. 19–26.

Thomas, J.T. (1991) Moutere Valley groundwater investigations 1989/1990. Unpublished Nelson Marlborough Regional report, 81 pp.

Thomas, J.T. (1992) Hydrogeology of the Moutere Valley with emphasis on groundwater recharge. Unpublished Tasman District Council report, 8 pp.

Thomas, J.T. (2001) Groundwater resources of the Tasman Region. *In* Groundwaters of New Zealand, M.R. Rosen and P.A. White (*eds*). New Zealand Hydrological Society Inc., Wellington. Pp. 411-425.